ORGANOMETALLICS
Article

Organometallics **2010,** *29,* 5215–5229 5215
DOI: 10.1021/om100522p

Niobaziridine Hydrides†

Joshua S. Figueroa, Nicholas A. Piro, Daniel J. Mindiola, Michael G. Fickes, and Christopher C. Cummins*

Department of Chemistry, Massachusetts Institute of Technology, Room 6-435, 77 Massachusetts Avenue, Cambridge, Massachusetts 02139-4307, United States

Received May 27, 2010

Presented herein are synthetic, structural, and reactivity studies delineating the characteristics of the niobaziridine hydride functional group as it pertains to the stabilization of trisanilide niobium complexes of the type Nb(N[R]Ar)$_3$ (**1**^{R}, Ar = 3,5-Me$_2$C$_6$H$_3$). Utilization of the *N*-isopropyl anilide ligand, N[*i*-Pr]Ar, results in the niobaziridine hydride dimer [Nb(H)(η^2-Me$_2$C═NAr)(N[*i*-Pr]Ar)$_2$]$_2$ ([**2**$^{i\text{-Pr}}$-H]$_2$). Dimer [**2**$^{i\text{-Pr}}$-H]$_2$ is thermally unstable at room temperature and decomposes via *ortho*-metalation and *i*-Pr radical ejection to a species containing a Nb−Nb bond. The ligand variant N[Np]Ar (Np = neopentyl) provides the room-temperature-stable niobaziridine hydride monomer Nb(H)(η^2-*t*-Bu(H)C═NAr)(N[Np]Ar)$_2$ (**2**^{Np}-H). Thermal decomposition of **2**^{Np}-H at elevated temperature (75 °C) provides the neopentyl imido complex Nb(NNp)(Ar)(N[Np]Ar)$_2$ (**5**^{Np}). H/D isotopic labeling studies provide evidence for reversible β-H elimination interconverting **2**^{Np}-H and its trisanilide tautomer [Nb(N[Np]Ar)$_3$] (**1**^{Np}), with the latter thereby implicated as an intermediate during the **2**^{Np}-H → **5**^{Np} conversion. Reactivity studies between **2**^{Np}-H and certain small-molecule substrates confirm that the niobaziridine hydride group can effectively mask a reactive d^2 Nb(III) trisanilide center. However, **2**^{Np}-H exhibits insertion chemistry when treated with a variety of unsaturated organic substrates, thus demonstrating a pronounced tendency to additionally function as a Lewis acidic, early transition metal hydride species. A general mechanism accounting for the divergent reactivity of **2**^{Np}-H is proposed. Niobaziridine hydride complexes derived from the amido ligands N[CH$_2$Ad]Ar, N[Cy]Ar, and NCy$_2$ (Ad = 1-adamantyl, Cy = cyclohexyl) are also presented, and their thermal behavior and reaction chemistry are compared with those of **2**^{Np}-H. In addition, the radical anion of **2**^{Np}-H is reported and compared with the neutral d^1 molybdaziridine hydride complex Mo(H)(η^2-Me$_2$C═NAr)(N[*i*-Pr]Ar)$_2$ (**3**$^{i\text{-Pr}}$-H), to which it is isoelectronic.

Introduction

Our interest in the chemistry of early metal trisanilide complexes, as exemplified by d^3 Mo(N[*t*-Bu]Ar)$_3$,[1−3] stems from their demonstrated ability to mediate novel activation profiles for small molecule substrates such as N$_2$,[4−7] P$_4$,[3,8,9] and CO$_2$.[10] To date, isolable examples of three-coordinate M(N[R]Ar)$_3$ complexes are known only for M = Ti,[11−13] V,[14−17] Cr,[18,19] and Mo;[1] also, a uranium analogue has been isolated as its THF adduct.[20] While the reactivity of trivalent M(N[R]Ar)$_3$ complexes of different periodic groups depends

† Part of the Dietmar Seyferth Festschrift.

*To whom correspondence should be addressed. E-mail: ccummins@mit.edu.

(1) Cummins, C. C. *Chem. Commun.* **1998**, 1777–1786.
(2) Laplaza, C. E.; Odom, A. L.; Davis, W. M.; Cummins, C. C.; Protasiewicz, J. D. *J. Am. Chem. Soc.* **1995**, *117*, 4999–5000.
(3) Cherry, J.-P. F.; Johnson, A. R.; Baraldo, L. M.; Tsai, Y.-C.; Cummins, C. C.; Kryatov, S. V.; Rybak-Akimova, E. V.; Capps, K. B.; Hoff, C. D.; Haar, C. M.; Nolan, S. P. *J. Am. Chem. Soc.* **2001**, *123*, 7271–7286.
(4) Laplaza, C. E.; Cummins, C. C. *Science* **1995**, *268*, 861–863.
(5) Laplaza, C. E.; Johnson, A. R.; Cummins, C. C. *J. Am. Chem. Soc.* **1996**, *118*, 709–710.
(6) Laplaza, C. E.; Johnson, M. J. A.; Peters, J. C.; Odom, A. L.; Kim, E.; Cummins, C. C.; George, G. N.; Pickering, I. J. *J. Am. Chem. Soc.* **1996**, *118*, 8623–8638.
(7) Peters, J. C.; Cherry, J.-P. F.; Thomas, J. C.; Baraldo, L.; Mindiola, D. J.; Davis, W. M.; Cummins, C. C. *J. Am. Chem. Soc.* **1999**, *121*, 10053–10067.
(8) Laplaza, C. E.; Davis, W. M.; Cummins, C. C. *Angew. Chem., Int. Ed. Engl.* **1995**, *34*, 2042–2044.
(9) Stephens, F. H.; Johnson, M. J. A.; Cummins, C. C.; Kryatova, O. P.; Kryatov, S. V.; Rybak-Akimova, E. V.; McDonough, J. E.; Hoff, C. D. *J. Am. Chem. Soc.* **2005**, *127*, 15191–15200.
(10) Mendiratta, A.; Cummins, C. C. *Inorg. Chem.* **2005**, *44*, 7319–7321.
(11) Wanandi, P. W.; Davis, W. M.; Cummins, C. C.; Russell, M. A.; Wilcox, D. E. *J. Am. Chem. Soc.* **1995**, *117*, 2110–2111.
(12) Peters, J. C.; Johnson, A. R.; Odom, A. L.; Wanandi, P. W.; Davis, W. M.; Cummins, C. C. *J. Am. Chem. Soc.* **1996**, *118*, 10175–10188.
(13) Agapie, T.; Diaconescu, P. L.; Mindiola, D. J.; Cummins, C. C. *Organometallics* **2002**, *21*, 1329–1340.
(14) Ruppa, K. B. P.; Desmangles, N.; Gambarotta, S.; Yap, G.; Rheingold, A. L. *Inorg. Chem.* **1997**, *36*, 1194–1197.
(15) Brask, J. K.; Fickes, M. G.; Sangtrirutnugul, P.; Durà-Vilà, V.; Odom, A. L.; Cummins, C. C. *Chem. Commun.* **2001**, 1676–1677.
(16) Brask, J. K.; Durà-Vilà, V.; Diaconescu, P. L.; Cummins, C. C. *Chem. Commun.* **2002**, 902–903.
(17) Agarwal, P.; Piro, N. A.; Meyer, K.; Müller, P.; Cummins, C. C. *Angew. Chem., Int. Ed.* **2007**, *46*, 3111–3114.
(18) Odom, A. L.; Cummins, C. C.; Protasiewicz, J. D. *J. Am. Chem. Soc.* **1995**, *117*, 6613–6614.
(19) Reardon, D.; Kovacs, I.; Ruppa, K. B. P.; Feghali, K.; Gambarotta, S.; Petersen, J. *Chem.—Eur. J.* **1997**, *3*, 1482–1488.
(20) Odom, A. L.; Arnold, P. L.; Cummins, C. C. *J. Am. Chem. Soc.* **1998**, *120*, 5836–5837.

Published on Web 10/15/2010

Scheme 1

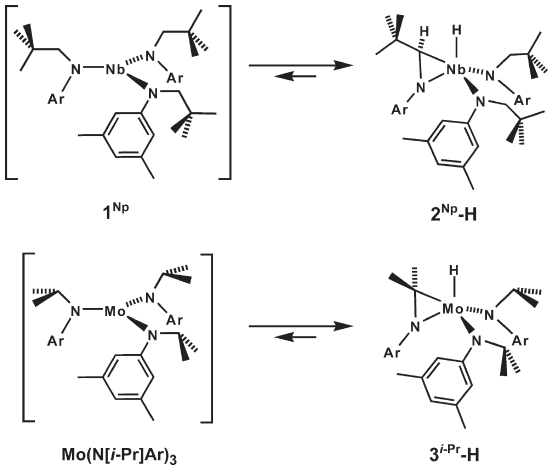

greatly on the d^n count, reactivity differences displayed by metals of the same group are governed by a less intuitive set of properties.[21−24] This point is highlighted by Mo(N[*t*-Bu]Ar)$_3$, which readily effects the reductive cleavage of the dinitrogen molecule,[4−7] while its Cr analogue, Cr(N[*t*-Bu]Ar)$_3$, is unreactive toward N_2 under similar conditions.[18] Accordingly, the discovery of new paradigms in small-molecule reactivity stemming from M(N[R]Ar)$_3$ complexes has fueled our quest to expand the library of known variants throughout the early transition elements.

In the last several years we have reported on the chemistry accessible to the d^2 niobium trisanilide fragment Nb(N[Np]Ar)$_3$ (**1**^{Np}, Np = neopentyl, Scheme 1), with specific attention being paid to its ability to activate the elemental forms of nitrogen and phosphorus.[25−29] These studies have resulted in a new phosphaalkyne synthesis[27] featuring metathetical C≡P triple-bond formation in a manner reminiscent of alkyne metathesis by Schrock-type alkylidynes.[30] In addition, we have developed an analogous organonitrile synthesis whereby the nitrogen atom of the new newly formed N≡C triple bond finds its origin in molecular nitrogen (N_2).[29] Most recently, the Nb(N[Np]Ar)$_3$ platform has allowed for P_2 transfer reactivity under mild solution-phase conditions, thus opening the door for utilization of this reactive diatomic unit in conventional synthesis.[31−33]

Unlike prototypical Mo(N[*t*-Bu]Ar)$_3$, Nb(N[Np]Ar)$_3$ does not exist as an isolable or kinetically persistent three-coordinate monomer. Our ability to employ the Nb(N[Np]Ar)$_3$ fragment for element activation chemistry stems from the finding that it can be effectively masked as a tautomeric niobaziridine hydride species, namely, Nb(H)(η^2-*t*-Bu(H)C=NAr)(N[Np]Ar)$_2$ (**2**^{Np}-H, Scheme 1).[25,34]

Despite its cyclometalated nature, niobaziridine hydride **2**^{Np}-H serves as a source of three-coordinate **1**^{Np} by virtue of reversible β-H elimination of the N[Np]Ar ligand. In general, tautomerization via reversible cyclometalation has emerged as a powerful and effective method for the stabilization of highly reactive, low-valent metal centers otherwise unavailable in free form. The recent work of Chirik,[35,36] and earlier studies by Bercaw,[37,38] has highlighted this fact in the context of cyclopentadienyl, alkyl, and aryl complexes of the early transition metals.

For three-coordinate M(N[R]Ar)$_3$ species, a similar masking strategy was reported by us with respect to the d^1 molybdaziridine hydride complex Mo(H)(η^2-Me$_2$C=NAr)(N[*i*-Pr]Ar)$_2$ (**3**$^{i\text{-}Pr}$-H, Scheme 1).[39] The latter functions as a synthon for three-coordinate Mo(N[*i*-Pr]Ar)$_3$, which is a less encumbered analogue of Mo(N[*t*-Bu]Ar)$_3$,[1] and accordingly effects N_2 cleavage[40,41] among other small-molecule activation processes.[39,42,43] The enthalpy of reaction to open the molybdaziridine ring of **3**$^{i\text{-}Pr}$-H was measured as 4.5 ± 0.3 kcal/mol by solution-phase calorimetry using thermodynamic paths related to nitrile binding studies.[44] Most interestingly however, **3**$^{i\text{-}Pr}$-H functions exclusively as a source of Mo(N[*i*-Pr]Ar)$_3$ and does not display reaction chemistry indicative of its metal-hydride formulation. This exclusivity is particularly important with respect to reactions with unsaturated organic substrates. Accordingly, ketones,[39] nitriles,[42] terminal alkynes,[43] and isocyanides[44] have all been shown to elicit C−H reductive elimination[44] in **3**$^{i\text{-}Pr}$-H, while insertion chemistry into its Mo−H bond has not been observed. Thus, the metallaziridine hydride functionality serves as an exceptionally reliable mask for a reactive three-coordinate trisanilide species in the case of molybdenum.

As communicated previously,[34] the reactivity of niobaziridine hydride **2**^{Np}-H with unsaturated organic functionality contrasts sharply with that of its molybdaziridine hydride analogue. While effectively serving as a source of **1**^{Np} in certain reactions, the Nb−H unit in **2**^{Np}-H has also been susceptible to insertion chemistry. Seeking to understand the

(21) Kuiper, D. S.; Wolczanski, P. T.; Lobkovsky, E. B.; Cundari, T. R. *Inorg. Chem.* **2008**, *47*, 10542–10553.
(22) Kuiper, D. S.; Douthwaite, R. E.; Mayol, A.-R.; Wolczanski, P. T.; Lobkovsky, E. B.; Cundari, T. R.; Lam, O. P.; Meyer, K. *Inorg. Chem.* **2008**, *47*, 7139–7153.
(23) Kuiper, D. S.; Wolczanski, P. T.; Lobkovsky, E. B.; Cundari, T. R. *Inorg. Chem.* **2008**, *47*, 10542–10553.
(24) Hirsekorn, K. F.; Hulley, E. B; Wolczanski, P. T.; Cundari, T. R. *J. Am. Chem. Soc.* **2008**, *130*, 1183–1196.
(25) Figueroa, J. S.; Cummins, C. C. *Dalton Trans.* **2006**, 2161–2168.
(26) Figueroa, J. S.; Cummins, C. C. *Angew. Chem., Int. Ed.* **2004**, *43*, 984–988.
(27) Figueroa, J. S.; Cummins, C. C. *J. Am. Chem. Soc.* **2004**, *126*, 13916–13917.
(28) Figueroa, J. S.; Cummins, C. C. *Angew. Chem., Int. Ed.* **2005**, *44*, 4592–4596.
(29) Figueroa, J. S.; Piro, N. A.; Clough, C. R.; Cummins, C. C. *J. Am. Chem. Soc.* **2006**, *128*, 940–950.
(30) Schrock, R. R. *Chem. Rev.* **2002**, *102*, 145–180.
(31) Piro, N. A.; Figueroa, J. S.; McKellar, J. T. *Science* **2006**, *313*, 1276–1279.
(32) Piro, N. A.; Cummins, C. C. *Inorg. Chem.* **2007**, *46*, 7387–7393.
(33) Piro, N. A.; Cummins, C. C. *J. Am. Chem. Soc.* **2008**, *130*, 9524–9535.
(34) Figueroa, J. S.; Cummins, C. C. *J. Am. Chem. Soc.* **2003**, *125*, 4020–4021.
(35) Pool, J. A.; Lobkovsky, E.; Chirik, P. J. *Organometallics* **2003**, *22*, 2797–2805.
(36) Pool, J. A.; Lobkovsky, E.; Chirik, P. J. *J. Am. Chem. Soc.* **2003**, *125*, 2241–2251.
(37) Parkin, G.; Bunel, E.; Burger, B. J.; Trimmer, M. S.; Van Asselt, A.; Bercaw, J. E. *J. Mol. Catal.* **1987**, *41*, 21–39.
(38) Van Asselt, A.; Trimmer, M. S.; Henling, L. M.; Bercaw, J. E. *J. Am. Chem. Soc.* **1988**, *110*, 8254–8255.
(39) Tsai, Y.-C.; Johnson, M. J. A.; Mindiola, D. J.; Cummins, C. C. *J. Am. Chem. Soc.* **1999**, *121*, 10426–10427.
(40) Cherry, J.-P. F.; Stephens, F. H.; Johnson, M. J. A.; Diaconescu, P. L.; Cummins, C. C. *Inorg. Chem.* **2001**, *40*, 6860–6862.
(41) Tsai, Y. C.; Cummins, C. C. *Inorg. Chim. Acta* **2003**, *345*, 63–69.
(42) Tsai, Y.-C.; Stephens, F. H.; Meyer, K.; Mendiratta, A.; Gheorghiu, M. D.; Cummins, C. C. *Organometallics* **2003**, *22*, 2902–2913.
(43) Tsai, Y.-C.; Diaconescu, P. L.; Cummins, C. C. *Organometallics* **2000**, *19*, 5260–5262.
(44) Stephens, F. H.; Figueroa, J. S.; Cummins, C. C.; Kryatova, O. P.; Kryatov, S. V.; Rybak-Akimova, E. V.; McDonough, J. E.; Hoff, C. D. *Organometallics* **2004**, *23*, 3126–3138.

Scheme 2

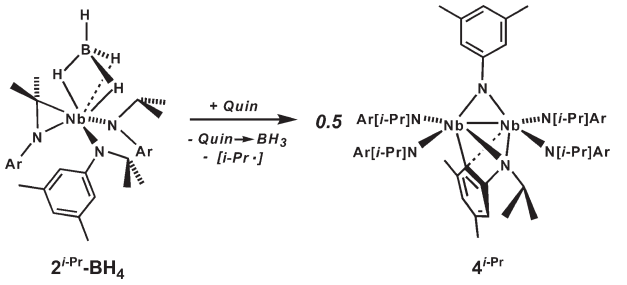

reactivity profile of $\mathbf{2}^{Np}$-H, with the aim of directing its reactivity toward that of the powerful two-electron reductant $\mathbf{1}^{Np}$, we have studied in greater detail the reaction chemistry of this system with a diverse host of substrates. Accordingly, in this contribution we present a more complete picture of the chemistry and solution behavior of $\mathbf{2}^{Np}$-H and several additional derivatives containing the niobaziridine hydride functionality.

Results and Discussion

Niobaziridine Hydride Formation with the *β*-H-Containing N[*i*-Pr]Ar Ligand. That a niobaziridine hydride complex could serve as a source of a reactive Nb-trisamide [$Nb(NR_2)_3$] fragment was first suggested to us by an intriguing report from Berno and Gambarotta.[45] Their treatment of $NbCl_4(THF)_2$ with three equivalents of the *β*-H-containing amide $LiNCy_2$ provided the niobaziridine chloride complex $Nb(Cl)(\eta^2\text{-}C_5H_{10}C{=}NCy)(NCy_2)_2$. The latter provided the bridging dinitrogen complex $(\mu_2\text{-}N_2)[Nb(NCy_2)_3]_2$ upon treatment with Na[$HBEt_3$] in the presence of N_2. Interestingly, the intermediacy of a niobaziridine hydride species was not proposed in this report. However, it is conceivable that H^- for Cl^- exchange provides the niobaziridine hydride complex $Nb(H)(\eta^2\text{-}C_5H_{10}C{=}NCy)(NCy_2)_2$, which is responsible for the observed N_2 chemistry by serving as a source of $Nb(NCy_2)_3$.

Inspired by this study, we set out to utilize the N[*i*-Pr]Ar ligand[39] for niobaziridine hydride formation. Previously, we had reported that treatment of $Nb(N[i\text{-}Pr]Ar)_3Cl_2$ with AgOTf and 5 equiv of $LiBH_4$ afforded the niobaziridine borohydride species $Nb(BH_4)(\eta^2\text{-}Me_2C{=}NAr)(N[i\text{-}Pr]Ar)_2$ ($\mathbf{2}^{i\text{-}Pr}$-BH_4, Scheme 2).[46] The latter is best viewed as a BH_3-trapped version of the desired target $Nb(H)(\eta^2\text{-}Me_2C{=}NAr)(N[i\text{-}Pr]Ar)_2$ ($\mathbf{2}^{i\text{-}Pr}$-H).

Unfortunately, borane abstraction from $\mathbf{2}^{i\text{-}Pr}$-BH_4 does not provide a straightforward route to $\mathbf{2}^{i\text{-}Pr}$-H. Instead, treatment of $\mathbf{2}^{i\text{-}Pr}$-BH_4 with the Lewis base quinuclidine (quin) led to the forest green complex $\mathbf{4}^{i\text{-}Pr}$ (Scheme 2), which has been formulated on the basis of crystallographic characterization.[47] Complex $\mathbf{4}^{i\text{-}Pr}$ is remarkable in that it is the product of not only Nb−Nb bond formation and *ortho*-metalation with formal H atom loss but also of *i*-Pr radical ejection from the N[*i*-Pr]Ar ligand. Notably, the two former ligand degradation modes have been observed by both Rothwell[48,49] and Gambarotta[50−53] in their investigations of low-valent Nb complexes supported by monoanionic aryloxide and amido ligands, respectively.

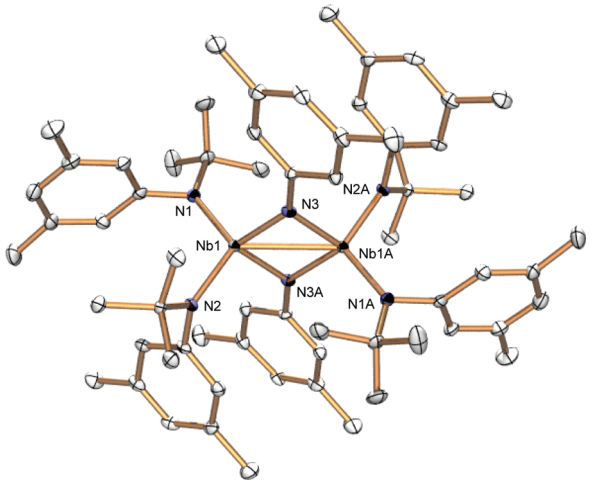

Figure 1. Molecular structure of $[(\mu\text{-}NAr)Nb(N[t\text{-}Bu]Ar)_2]_2$. Selected bond distances (Å) and angles (deg): Nb(1)−Nb(1A) = 2.7594(13); Nb(1)−N(1) = 2.041(6); Nb(1)−N(2) = 2.022(5); Nb1−N(3) = 1.977(6); Nb(1)−Nb(3A) = 2.023(6); Nb(1)−N(3)−Nb(1A) = 87.2(2); N(3)−Nb(1)−N(3A) = 92.8(2); N(1)−Nb(1)−N(3) = 114.7(2).

Scheme 3

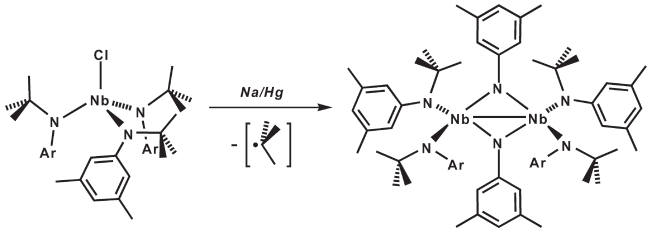

For radical ejection, it is pertinent that this ligand degradation pathway is also the primary mode of decomposition for N[*t*-Bu]Ar-ligated Nb systems. Accordingly, our attempts to prepare the three-coordinate complex $Nb(N[t\text{-}Bu]Ar)_3$ by chemical reduction of the Nb(IV) monochloride complex $Nb(Cl)[N[t\text{-}Bu]Ar)_3$ have invariably resulted in the formation of the bridging bis-imido dimer $[(\mu\text{-}NAr)Nb(N[t\text{-}Bu]Ar)_2]_2$ (Scheme 3, Figure 1). Formation of $[(\mu\text{-}NAr)Nb(N[t\text{-}Bu]Ar)_2]_2$ is proposed to occur by a multistep process in which putative $[Nb(N[t\text{-}Bu]Ar)_3]$ is formed upon reduction and elicits the ejection of *tert*-butyl radical,[54] concomitant with the formation of the Nb^{IV} imido species $[Nb(NAr)(N[t\text{-}Bu]Ar)_2]$. The latter is thought to rapidly dimerize with Nb−Nb bond formation to the observed product. Furthermore, the relatively large size of the remaining *t*-Bu substituents in $[(\mu\text{-}NAr)Nb(N[t\text{-}Bu]Ar)_2]_2$ may presumably

(45) Berno, P.; Gambarotta, S. *Organometallics* **1995**, *14*, 2159–2161.
(46) Mindiola, D. J.; Cummins, C. C. *Organometallics* **2001**, *20*, 3626–3628.
(47) Mindiola, D. J. Ph.D. Thesis, Department of Chemistry, Massachusetts Institute of Technology, Cambridge, MA, 2000.
(48) Steffey, B. D.; Chesnut, R. W.; Kerschner, J. L.; Pellechia, P. J.; Fanwick, P. E.; Rothwell, I. P. *J. Am. Chem. Soc.* **1989**, *111*, 378–380.
(49) Chesnut, R. W.; Jacob, G. G.; Yu, J. S.; Fanwick, P. E.; Rothwell, I. P. *Organometallics* **1991**, *10*, 321–328.
(50) Tayebani, M.; Kasani, A.; Feghali, K.; Gambarotta, S.; Bensimon, C. *Chem. Commun.* **1997**, 2001–2002.
(51) Tayebani, M.; Feghali, K.; Gambarotta, S.; Yap, G. *Organometallics* **1998**, *17*, 4282–4290.
(52) Tayebani, M.; Gambarotta, S.; Yap, G. *Organometallic* **1998**, *17*, 3639–3641.
(53) Tayebani, M.; Feghali, K.; Gambarotta, S.; Bensimon, C. *Organometallics* **1997**, *16*, 5084–5088.
(54) For thermally induced *t*-Bu radical ejection stemming from d^1 (E)Mo(N[*t*-Bu]Ar)$_3$ complexes (E = O, S, Se, Te), see: Johnson, A. R.; Davis, W. M.; Cummins, C. C.; Serron, S.; Nolan, S. P.; Musaev, D. G.; Morokuma, K. *J. Am. Chem. Soc.* **1998**, *120*, 2071–2085.

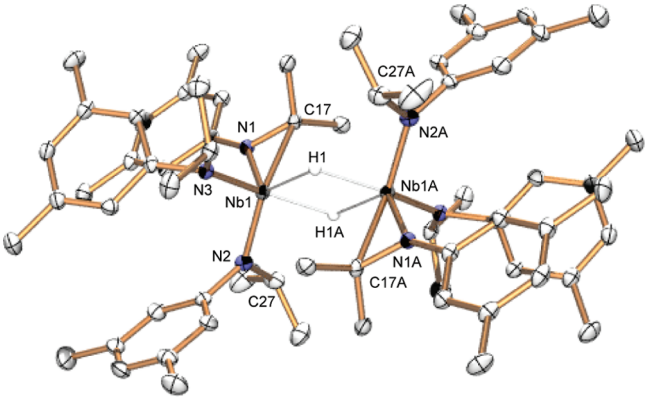

Figure 2. Molecular structure of $[2^{i\text{-Pr}}\text{-H}]_2$. Selected bond distances (Å): Nb(1)−H(1) = 1.802(6); Nb(1)−H(1A) = 1.987(6); Nb(1)−Nb(1A) = 3.301(8); Nb(1)−N(1) = 1.948(3); Nb(1)−C(37) = 2.248(4); Nb(1)−N(2) = 2.013(3); N(1)−C(37) = 1.408(5); N(2)−C(27) = 1.482(5).

Scheme 4

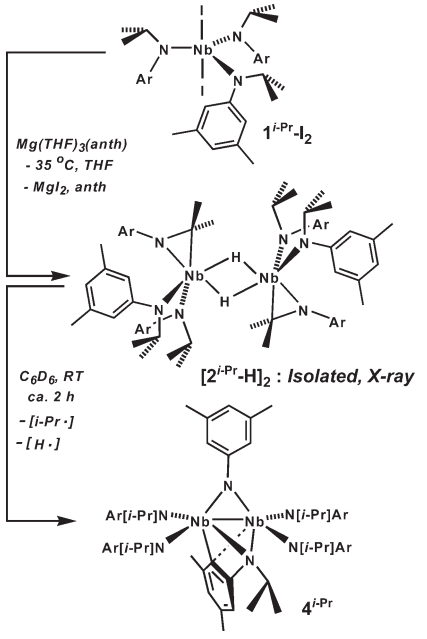

account for a retardation of additional ligand activation process, as compared to the N[*i*-Pr]Ar system of $\mathbf{4}^{i\text{-Pr}}$.

In the N[*i*-Pr]Ar-ligated Nb system, complex $\mathbf{4}^{i\text{-Pr}}$ is also the major product obtained when the Nb(V) dihalides $Nb(Cl)_2(N[i\text{-Pr}]Ar)_3$[55] and $Nb(I)_2(N[i\text{-Pr}]Ar)_3$[56] are combined with strong reductants such as Na/Hg and KC_8.[57] Contrastingly, treatment of $Nb(I)_2(N[i\text{-Pr}]Ar)_3$ with the relatively mild reducing agent $Mg(THF)_3$(anthracene),[58] followed by a rapid, low-temperature workup, successfully provides niobaziridine hydride $\mathbf{2}^{i\text{-Pr}}$-H as a dark orange solid (Scheme 4). Consistent with its formulation, diamagnetic $\mathbf{2}^{i\text{-Pr}}$-H displays a C_s-symmetric pattern of N[*i*-Pr]Ar resonances in its ^{1}H NMR spectrum (C_6D_6). However, crystallographic analysis revealed that it exists as a centrosymmetric, dihydrido-bridged dimer in the solid state (Figure 2). This dimeric nature of $\mathbf{2}^{i\text{-Pr}}$-H is particularly surprising given that the monomeric solid-state structure of the d^1 molybdaziridine hydride $\mathbf{3}^{i\text{-Pr}}$-H has been unequivocally established by both X-ray and neutron diffraction.[39] Evidently the steric properties of the N[*i*-Pr]Ar ligand are insufficient to preclude dimerization of niobaziridine hydride complexes derived from it. Therefore, the contrasting solid-state structures point strikingly to the differences in d^n configuration between $\mathbf{2}^{i\text{-Pr}}$-H and $\mathbf{3}^{i\text{-Pr}}$-H, with the d^0 nature of $\mathbf{2}^{i\text{-Pr}}$-H rendering it much more Lewis acidic than its Mo counterpart (*vide infra*).

Critical to the isolation of $\mathbf{2}^{i\text{-Pr}}$-H is the low-temperature workup that must be employed. Once isolated, $\mathbf{2}^{i\text{-Pr}}$-H is thermally unstable in solution and decomposes to dimer $\mathbf{4}^{i\text{-Pr}}$ over the course of ca. 2 h at room temperature (Scheme 4). While the instability of $\mathbf{2}^{i\text{-Pr}}$-H prevented an accurate determination of its degree of aggregation in solution, the formation of $\mathbf{4}^{i\text{-Pr}}$ points strongly to the possibility that the dimeric structure as observed in the solid state may be preserved. Furthermore, formation of a reactive d^2 $[Nb(N[i\text{-Pr}]Ar)_3]$ fragment via reversible β-H elimination from one or both niobaziridine hydride units in dimeric $\mathbf{2}^{i\text{-Pr}}$-H may account for the observed ligand degradation processes leading to $\mathbf{4}^{i\text{-Pr}}$.

Monomeric Niobaziridine Hydride Formation with the β-H-Containing N[Np]Ar Ligand. Evidence for Reversible β-H Elimination in Solution. To combat the limitations of the N[*i*-Pr]Ar ligand, we reasoned that a thermally robust niobaziridine hydride might be obtained if a ligand resistant to radical ejection was employed. Therefore, the β-H-containing anilido ligand N[Np]Ar was selected due to the greater thermodynamic barrier to neopentyl radical formation than that for either the isopropyl or *tert*-butyl radical.[59] In addition, it was thought that three neopentyl substituents would likely impart the necessary steric protection to engender the formation of a monomeric niobaziridine hydride. This postulate was confirmed with the successful synthesis[34] of the kinetically persistent niobaziridine hydride $\mathbf{2}^{Np}$-H via reduction of $NbX_2(N[Np]Ar)_3$ precursors (X = I[34] or OSO_2CF_3[25,27]) with $Mg(THF)_3$(anthracene). Furthermore, X-ray diffraction has revealed that $\mathbf{2}^{Np}$-H indeed exists as a discrete monomer in the solid state (Figure 3).[34]

Diamagnetic niobaziridine hydride $\mathbf{2}^{Np}$-H retains its integrity as an orange crystalline solid for months when stored at low temperature (−35 °C). However, when dissolved in C_6D_6, $\mathbf{2}^{Np}$-H is observed to decay slowly and irreversibly at room temperature ($t_{1/2} \approx 4.5$ d) to its neopentylimido isomer, $Nb(NNp)(Ar)(N[Np]Ar)_2$ ($\mathbf{5}^{Np}$, Scheme 5). Importantly, radical ligand degradation processes are not observed when utilizing the N[Np]Ar ligand with Nb. Therefore, the formation of $\mathbf{5}^{Np}$ can be rationalized by a sequence involving (i) reversible β-H elimination from $\mathbf{2}^{Np}$-H leading to the reactive three-coordinate species $\mathbf{1}^{Np}$, followed by (ii) two-electron C−N oxidative addition of an intact N[Np]Ar ligand by the latter (Scheme 5). While the observation of facile C−N bond rupture implies that d^2 $\mathbf{1}^{Np}$ is accessible in solution, direct spectroscopic evidence for such a species has not been obtained during the $\mathbf{2}^{Np}$-H to $\mathbf{5}^{Np}$ conversion.

(55) Mindiola, D. J.; Meyer, K.; Cherry, J.-P. F.; Baker, T. A.; Cummins, C. C. *Organometallics* **2000**, *19*, 1622–1624.
(56) Experimental details are provided in the Supporting Information.
(57) Schwindt, M. A.; Lejon, T.; Hegedus, L. S. *Organometallics* **1990**, *9*, 2814–2819.
(58) Freeman, P. K.; Hutchinson, L. L. *J. Org. Chem.* **1983**, *48*, 879.
(59) Heats of formation (ΔH^o_f, kcal/mol) for the following radicals scale as *tert*-C_4H_9 (7.6 ± 1.2) < *iso*-C_3H_7 (18.2 ± 1.5) < neo-C_5H_{11} (30.0 ± 1.0) . *CRC Handbook of Chemistry and Physics*, 67th ed.; CRC Press: Boca Raton, FL, 1987.

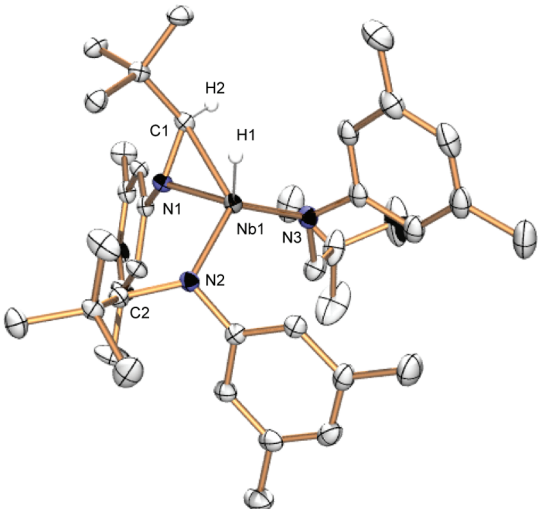

Figure 3. Molecular structure of $\mathbf{2}^{Np}$-H.

Scheme 5

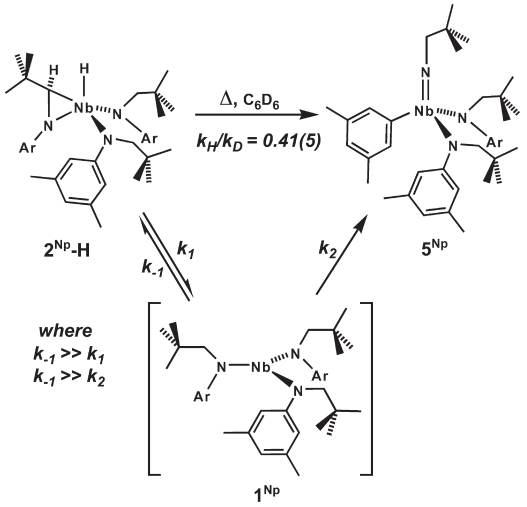

In order to further probe for the formation of $\mathbf{1}^{Np}$ in solution, the decay of $\mathbf{2}^{Np}$-H and its selectively labeled niobaziridine deuteride isotopomer, Nb(D)(η^2-*t*-Bu(D)C=NAr)(N[Np-d_2]Ar)$_2$ ($\mathbf{2}^{Np}$-D; Np-d_2 = CD_2(*t*-Bu)),[60] were measured as a function of time. For both $\mathbf{2}^{Np}$-H and $\mathbf{2}^{Np}$-D, clean, reproducible first-order kinetics were obtained at 75 °C (C_6D_6), resulting in a system characterized by a significant observed inverse isotope effect (k_H/k_D = 0.41(5)).[61,62] Such an observed isotope effect is consistent with the rapid interconversion of $\mathbf{2}^{Np}$-H and three-coordinate $\mathbf{1}^{Np}$ via reversible β-H elimination (k_1/k_{-1}, Scheme 5) and finds analogy with alkane elimination studies from $L_nM(H)(R)$ complexes, which likewise result in the formation of reactive, coordinatively unsaturated metal fragments.[61−66] Furthermore, the formation of imido $\mathbf{5}^{Np}$ is interpreted to result from a slower C−N bond cleavage process, which serves to irreversibly trap $\mathbf{1}^{Np}$ in the absence of a C−H activation event (k_2, Scheme 5).[67,68]

Whereas the isotopic labeling results strongly suggest that three-coordinate $\mathbf{1}^{Np}$ interchanges $\mathbf{2}^{Np}$-H and $\mathbf{5}^{Np}$, it is at best a fleeting species. Due to its reactive nature, $\mathbf{1}^{Np}$ is likely stabilized by agostic C−H[69,70] and/or π-arene interactions[71,72] from the N[Np]Ar ligand and never present in free form. Indeed, evidence for π-arene interactions in d^2 group 5 M(N[R]Ar)$_3$ complexes can be garnered from the molecular structure of V(N[1-Ad]Ar)$_3$,[14] in which a single anilido ligand binds in an η^3-($N-C_{ipso}-C_{ortho}$) fashion. Thus, we suggest that the latter structural feature, as observed for V(N[1-Ad]Ar)$_3$, can be considered as a snapshot of the C−N cleavage process involving the reactive $\mathbf{1}^{Np}$ fragment.

Imido $\mathbf{5}^{Np}$ is stable for extended periods at elevated temperature, thus rendering it the thermodynamic product relative to niobaziridine hydride $\mathbf{2}^{Np}$-H. This notion has been substantiated by DFT calculations performed on the hypothetical niobaziridine hydride Nb(H)(η^2-Me(H)C=NPh)(NH$_2$)$_2$ (**2m**-H), which is calculated to lie ca. 29 kcal/mol higher in energy than its ethyl imido isomer Nb(NEt)(Ph)(NH$_2$)$_2$ (**5m**). This remarkable discrepancy highlights the kinetic formation of the niobaziridine hydride functionality from $\mathbf{1}^{Np}$ via C−H activation, when C−N oxidative addition is clearly energetically preferred. Furthermore, the marked ability of putative low-valent Nb species to activate C−N bonds in organoamide ligands has been documented by Gambarotta for several NR_2 derivatives.[50,52,53] Accordingly, such rampant C−N activation capability further punctuates the ability of the niobaziridine hydride unit, as derived from the N[Np]Ar ligand, to impart kinetic stabilization to the reactive $\mathbf{1}^{Np}$ fragment in solution.

Divergent Reactivity of Niobaziridine Hydride $\mathbf{2}^{Np}$-H with Small-Molecule Substrates. Atom Abstraction and Complexation vs Hydride Transfer. The prolonged stability of $\mathbf{2}^{Np}$-H in solution has allowed for a detailed survey of its reactivity toward small-molecule substrates. We have shown[34] that $\mathbf{2}^{Np}$-H readily generates the terminal chalcogenido[73] species (E)Nb(N[Np]Ar)$_3$ ($\mathbf{1}^{Np}$-E, E = O, S, Se, Te), when treated with suitable chalcogen-atom sources. In addition, treatment of $\mathbf{2}^{Np}$-H with mesitylnitrile (MesCN, Mes = 2,4,6-Me$_3$C$_6$H$_2$) leads to the exclusive formation of the η^2-nitrile complex (η^2-MesCN)Nb(N[Np]Ar)$_3$ ($\mathbf{1}^{Np}$-NCMes).[34] Accordingly, the formation of complexes $\mathbf{1}^{Np}$-E and $\mathbf{1}^{Np}$-NCMes, which contain three intact N[Np]Ar ligands, demonstrates that the niobaziridine hydride functionality of $\mathbf{2}^{Np}$-H is indeed capable of reversible β-H elimination upon reaction with incoming substrates.

Of these latter reactions, the clean and irreversible formation of the terminal oxo complex (O)Nb(N[Np]Ar)$_3$ ($\mathbf{1}^{Np}$-O)

(60) Proton incorporation into the methylene-d_2 positions in $\mathbf{2}^{Np}$-D is not observed by ^{1}H NMR spectroscopy (C_6D_6), thereby ruling out a complicated, Nb-mediated exchange process between all C−H bonds of the N[Np]Ar ligand framework.

(61) Jones, W. D. *Acc. Chem. Res.* **2003**, *36*, 140–146.
(62) Churchill, D. G.; Janak, K. E.; Wittenberg, J. S.; Parkin, G. *J. Am. Chem. Soc.* **2003**, *125*, 1403–1420.
(63) Janowicz, A. H.; Bergman, R. G. *J. Am. Chem. Soc.* **1982**, *104*, 352–354.
(64) Buchanan, J. M.; Stryker, J. M.; Bergman, R. G. *J. Am. Chem. Soc.* **1986**, *108*, 1537–1550.
(65) Periana, R. A.; Bergman, R. G. *J. Am. Chem. Soc.* **1986**, *108*, 7332–7346.
(66) Parkin, G.; Bercaw, J. E. *Organometallics* **1989**, *8*, 1172–1179.
(67) Bullock, R. M.; Headford, C. E. L.; Hennessy, K. M.; Kegley, S. E.; Norton, J. R. *J. Am. Chem. Soc.* **1989**, *111*, 3897–3908.
(68) Gould, G. L.; Heinekey, D. M. *J. Am. Chem. Soc.* **1989**, *111*, 5502–5504.
(69) Brookhart, M.; Green, M. L. H. *J. Organomet. Chem.* **1983**, *250*, 395–408.
(70) Brookhart, M.; Green, M. L. H.; Wong, L. L. *Prog. Inorg. Chem.* **1988**, *36*, 1–124.
(71) Belt, S. T.; Dong, L.; Duckett, S. B.; Jones, W. D.; Partridge, M. G.; Perutz, R. N. *Chem. Commun.* **1991**, 266–269.
(72) Reinartz, S.; White, P. S.; Brookhart, M.; Templeton, J. L. *J. Am. Chem. Soc.* **2001**, *123*, 12724–12725.
(73) Parkin, G. *Prog. Inorg. Chem.* **1998**, *47*, 1–165.

Scheme 6

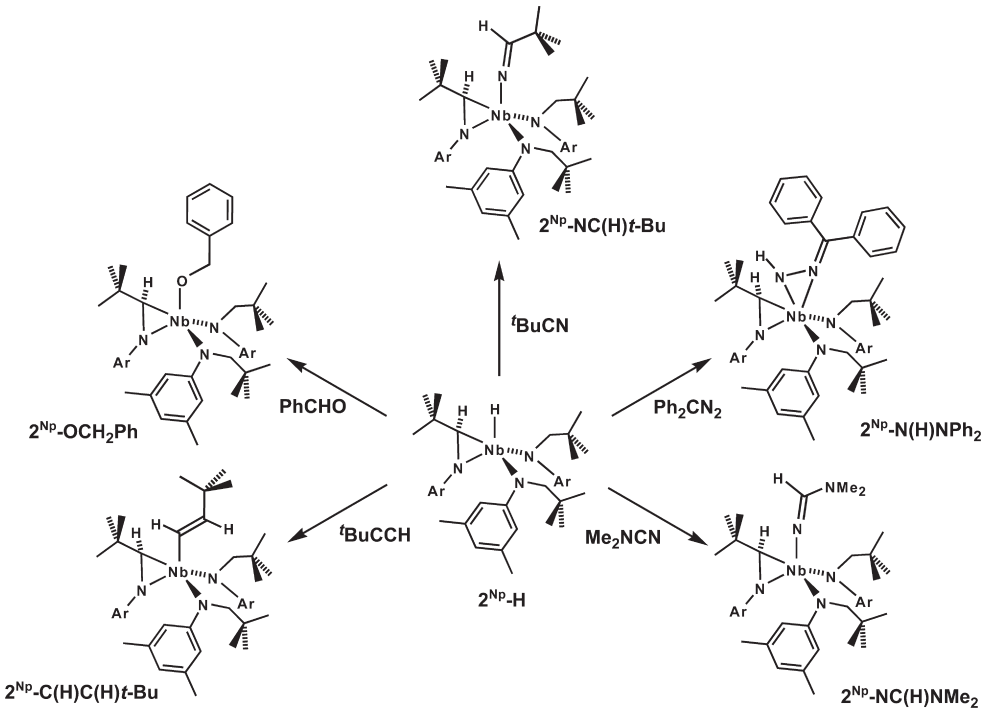

Table 1. $OPPh_3$ Concentration (M) and Observed Rate Constants (k_{obs}, s^{-1}) for the Deoxygenation of $OPPh_3$ by 2^{Np}-H (C_6D_6, 20 °C) under Pseudo-First-Order Conditions

$[OPPh_3]$	equivalents	k_{obs}
0.15	10	$2.7(1) \times 10^{-4}$
0.23	15	$5.9(2) \times 10^{-4}$
0.30	20	$5.5(3) \times 10^{-4}$
0.38	25	$6.0(3) \times 10^{-4}$
0.45	30	$5.4(4) \times 10^{-4}$

by treatment of 2^{Np}-H with triphenylphosphine oxide ($OPPh_3$) is particularly noteworthy.[34] Well-characterized examples of the deoxygenation of phosphine oxides by transition metal complexes are rare,[74] with the reports of Mayer[75] and Wolczanski[76,77] serving as precedent. In both the latter cases, reactive low-valent early transition metal complexes were utilized for the cleavage of the phosphoryl P=O bond, which lends further credence to the notion that 2^{Np}-H can function as the masked equivalent of three-coordinate 1^{Np}. For the deoxygenation of $OPPh_3$ by 2^{Np}-H, preliminary measurements by ^{1}H NMR spectroscopy indicate that the system adheres to smooth pseudo-first-order kinetics in C_6D_6 before reaching a saturation point in $[OPPh_3]$ at ca. 0.23 M (Table 1).

Despite exhibiting reversible β-H elimination as illustrated above, 2^{Np}-H displays a second reactivity pattern, which has revealed its tendency to additionally function as a Lewis acidic early metal hydride. For example, treatment of 2^{Np}-H with *tert*-butylnitrile (*t*-BuCN) results in the formation of the ketimido complex Nb(N=C(H)*t*-Bu)(η^2-*t*-Bu(H)C=NAr)(N[Np]Ar)$_2$ (2^{Np}-NC(H)*t*-Bu, Scheme 6, top), which features an unperturbed niobaziridine ring as determined by X-ray crystallography.[34] Complex 2^{Np}-NC(H)*t*-Bu can be viewed as the product of *t*-BuCN insertion[78] into the Nb−H bond of 2^{Np}-H and provides a striking contrast to the behavior observed with MesCN. Furthermore, insertion into the Nb−H unit of 2^{Np}-H is not limited specifically to *t*-BuCN. As depicted in Scheme 6, a diverse array of organic substrates behave similarly,[79] thus revealing that insertion chemistry is pronounced for the niobaziridine hydride functionality in 2^{Np}-H.

Notably, the ability to insert an organic functionality appears to be generally characteristic of the niobaziridine hydride group. For the N[*i*-Pr]Ar-containing system, we have previously reported the synthesis of the niobaziridine alkoxide complex Nb(OC(H)Ph$_2$)(η^2-Me$_2$C=NAr)(N[*i*-Pr]Ar)$_2$ ($2^{i\text{-Pr}}$-OC(H)Ph$_2$) from treatment of the borohydride complex $2^{i\text{-Pr}}$-BH_4 with quinuclidine in the presence of benzophenone.[46] In this latter case, the highly Lewis acidic monomer $2^{i\text{-Pr}}$-H is presumably formed via sequential borane abstraction/benzophenone insertion without competing formation of dimer $4^{i\text{-Pr}}$. Thus while the steric demands of the N[Np]Ar ligand serve to prevent dimerization of 2^{Np}-H, its Nb center remains highly Lewis acidic, serving to impart substantial nucleophilic character to the hydride unit.

Although the insertion of substrates by 2^{Np}-H removes the hydride moiety, the niobaziridine ring remains active for

(74) Typically the reverse reaction, namely, transfer of a terminal oxo moiety to phosphine, is encountered; see: (a) Holm, R. H. *Chem. Rev.* **1987**, *87*, 1401–1449. (b) Holm, R. H.; Donahue, J. P. *Polyhedron* **1993**, *12*, 571–589.

(75) Brock, S. L.; Mayer, J. M. *Inorg. Chem.* **1991**, *30*, 2138–2143.

(76) Veige, A. S.; Slaughter, L. M.; Wolczanski, P. T.; Matsunaga, N.; Decker, S. A.; Cundari, T. R. *J. Am. Chem. Soc.* **2001**, *123*, 6419–6420.

(77) Veige, A. S.; Slaughter, L. M.; Lobkovsky, E.; Wolczanski, P. T.; Matsunaga, N.; Decker, S. A.; Cundari, T. R. *Inorg. Chem.* **2003**, *42*, 6204–6224.

(78) For examples of organonitrile insertion into early transition metal and lanthanide hydrides, see: (a) Churchill, M. R.; Wasserman, H. J.; Belmonte, P. A.; Schrock, R. R. *Organometallics* **1982**, *1*, 559–561. (b) Evans, W. J.; Meadows, J. H.; Hunter, W. E.; Atwood, J. L. *J. Am. Chem. Soc.* **1984**, *106*, 1291–1300. (c) Alelyunas, Y. W.; Guo, Z.; LaPointe, R. E.; Jordan, R. F. *Organometallics* **1993**, *12*, 544–553.

(79) α-H insertion of N_2CPh_2 into early transition metal hydride complexes has been reported previously; see: Gambarotta, S.; Floriani, C.; Chiesi-Villa, A.; Guastini, C. *Inorg. Chem.* **1983**, *22*, 2029–2034.

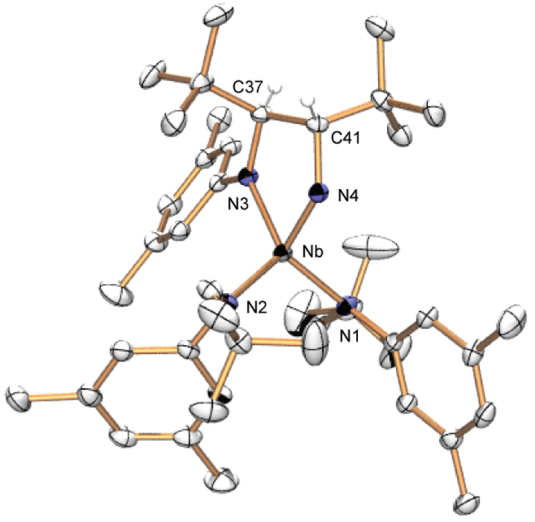

Figure 4. Molecular structure of $\mathbf{6}^{Np}$-*t*-Bu. Selected bond distances (Å) and angles (deg): Nb(1)−N(4) = 1.759(2), Nb(1)−N(3) = 2.017, C(37)−C(41) = 1.560(4), Nb(1)−N(4)−C(41) = 128.6(2).

Scheme 7

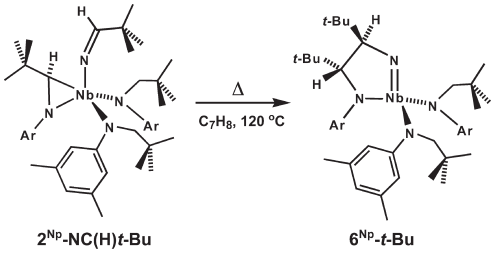

additional chemistry. Accordingly, the ketimido complex $\mathbf{2}^{Np}$-NC(H)*t*-Bu cleanly undergoes ring expansion to its tethered imido[80] isomer $\mathbf{6}^{Np}$-*t*-Bu when heated at 120 °C in toluene solution (Scheme 7). This complex, with its imido tethered in a five-membered ring, displays an unusually small Nb−N−C angle of 128.6(2)° at the imido nitrogen. Similarly small metrics are found for the Nb−N−Nb angles of 129−131° in the six-membered rings of $[(Ar[^{i}Pr]N)_2Nb{=}N]_3$,[55] while an angle of 151° has been reported for the Nb−N−C angle $(\eta^5\text{-}C_5H_4)(CH_2)_3NNbCl_2PMe_3$.[81] The formation of complex $\mathbf{6}^{Np}$-*t*-Bu (Figure 4) likely arises via intramolecular nucleophilic attack by the niobaziridine carbon on the ketimido ligand in $\mathbf{2}^{Np}$-NC(H)*t*-Bu. Notably, early transition metal metallaziridine complexes are well known to elicit nucleophilic C−C bond formation with unsaturated substrates.[82−87] An analogous ring expansion process is also observed in the reaction between $\mathbf{2}^{Np}$-H and

(80) Gountchev, T. I.; Tilley, T. D. *J. Am. Chem. Soc.* **1997**, *119*, 12831–12841.
(81) Antonelli, D. M.; Greem, M. L. H.; Mountford, P. *J. Organomet. Chem.* **1992**, *438*, C4.
(82) Roskamp, E. J.; Pedersen, S. F. *J. Am. Chem. Soc.* **1987**, *109*, 6551–6553.
(83) Buchwald, S. L.; Lucas, E. A.; Davis, W. M. *J. Am. Chem. Soc.* **1989**, *111*, 397–398.
(84) Buchwald, S. L.; Watson, B. T.; Wannamaker, M. W.; Dewan, J. C. *J. Am. Chem. Soc.* **1989**, *111*, 4486–4494.
(85) Gately, D. A.; Norton, J. R.; Goodson, P. A. *J. Am. Chem. Soc.* **1995**, *117*, 986–996.
(86) Gately, D. A.; Norton, J. R. *J. Am. Chem. Soc.* **1996**, *118*, 3479–3489.
(87) Tunge, J. A.; Czerwinski, C. J.; Gately, D. A.; Norton, J. R. *Organometallics* **2001**, *20*, 254–260.

Scheme 8

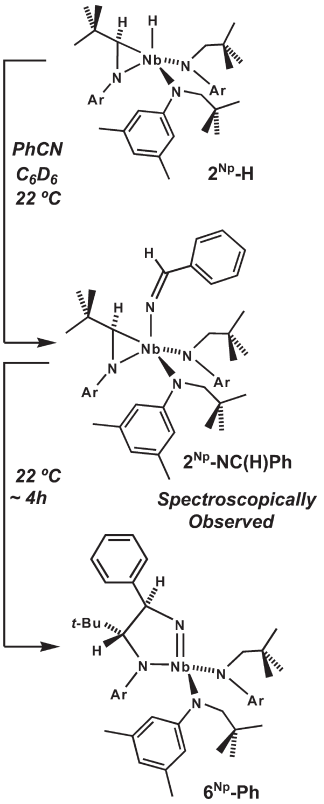

benzonitrile (PhCN). Thus treatment of C_6D_6 solutions of $\mathbf{2}^{Np}$-H with PhCN at room temperature rapidly generates the ketimido complex $\mathbf{2}^{Np}$-NC(H)Ph as an observable intermediate by ^{1}H NMR spectroscopy.[88] The latter smoothly decays *without heating* to the tethered imido complex $\mathbf{6}^{Np}$-Ph over the course of ca. 4 h (Scheme 8), thereby indicating that the thermal stability of $\mathbf{2}^{Np}$-NC(H)*t*-Bu results in part from its sterically encumbering ketimido *t*-Bu substituent.

It is worthy of mention that the niobaziridine rings in complexes $\mathbf{2}^{Np}$-NC(H)*t*-Bu and $\mathbf{2}^{Np}$-NC(H)Ph preferentially attack at the ketimide sp^2 carbon, despite the fact that the ketimide ligand also features an accessible *β*-H atom. While *β*-H abstraction by the niobaziridine ring can conceivably furnish the corresponding η^2-nitrile isomers of $\mathbf{2}^{Np}$-NC(H)*t*-Bu and $\mathbf{2}^{Np}$-NC(H)Ph (i.e., $(\eta^2\text{-}t\text{-BuCN})Nb(N[Np]Ar)_3$ and $(\eta^2\text{-PhCN})Nb(N[Np]Ar)_3$), this pathway is evidently disfavored. The same is true of complexes $\mathbf{2}^{Np}$-OCH_2Ph, $\mathbf{2}^{Np}$-C(H)C(H)*t*-Bu, and $\mathbf{2}^{Np}$-$NC(H)NMe_2$ (Scheme 6), which all retain their integrity for extended periods at elevated temperatures (120 °C, 3 d, C_7D_8). Again, similar behavior was observed with the niobaziridine alkoxide complex $\mathbf{2}^{i\text{-}Pr}$-$OC(H)Ph_2$, which did not interconvert thermally with the independently prepared η^2-benzophenone complex $(\eta^2\text{-}Ph_2CO)Nb(N[i\text{-}Pr]Ar)_3$ ($\mathbf{1}^{i\text{-}Pr}$-$OCPh_2$) via *β*-H abstraction.[46] Furthermore, for the N[Np]Ar system, it is notable that ketimide $\mathbf{2}^{Np}$-$NC(H)NMe_2$ does not undergo ring expansion when heated. This circumstance for $\mathbf{2}^{Np}$-$NC(H)NMe_2$ is likely due to electronic saturation of the sp^2 ketimido carbon by its pendant amino group.[89]

(88) Complex $\mathbf{2}^{Np}$-NC(H)Ph is characterized by a well-resolved, diagnostic aldehydic-type proton resonance centered at *δ* 9.57 ppm, which is observed to decay over time.
(89) Spectroscopic evidence for this notion is provided from the ^{1}H NMR spectrum of $\mathbf{2}^{Np}$-$NC(H)NMe_2$, where the amino-methyl groups appear as distinct singlets at room temperature, thus indicating hindered rotation.

Scheme 9

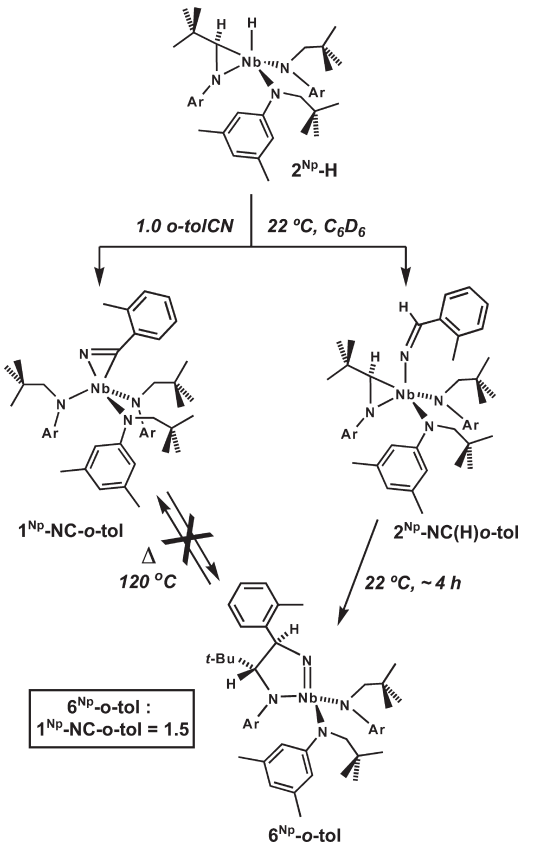

The fact that MesCN exclusively forms the η^2-nitrile complex $\mathbf{1}^{Np}$-NCMes and that β-H abstraction is not observed for complexes $\mathbf{2}^{Np}$-NC(H)R (R = *t*-Bu, Ph, NMe_2) suggests that dual pathways of reactivity are accessible to niobaziridine hydride $\mathbf{2}^{Np}$-H depending on the nature of the *substrate*. This notion is further substantiated by the reactivity observed between $\mathbf{2}^{Np}$-H and *ortho*-tolylnitrile (*o*-tolCN). Remarkably, treatment of $\mathbf{2}^{Np}$-H with one equivalent of *o*-tolCN at room temperature leads rapidly to the formation of *both* the ketimide $\mathbf{2}^{Np}$-NC(H)*o*-tol and the η^2-nitrile complex $\mathbf{1}^{Np}$-NC-*o*-tol in a 1:1.5 ratio, as determined by ^{1}H NMR spectroscopy (Scheme 9). Over the course of 5 h, $\mathbf{2}^{Np}$-NC(H)*o*-tol converts to imido $\mathbf{6}^{Np}$-*o*-tol while maintaining an overall ($\mathbf{2}^{Np}$-NC-*o*-tol + $\mathbf{6}^{Np}$-*o*-tol):$\mathbf{1}^{Np}$-NC-*o*-tol ratio of 1.5:1. Extended heating of the resultant $\mathbf{6}^{Np}$-*o*-tol + $\mathbf{1}^{Np}$-NC-*o*-tol mixture did not affect the relative product distribution (120 °C, ca. 1 week), thus indicating distinct pathways of formation[90] for $\mathbf{1}^{Np}$-NC-*o*-tol and $\mathbf{2}^{Np}$-NC(H)*o*-tol from $\mathbf{2}^{Np}$-H. To this end, it is clear that the *ortho* methyl groups of the substituted benzonitriles MesCN and *o*-tolCN play a critical role in dictating the behavior of $\mathbf{2}^{Np}$-H. As elaborated upon below, we believe such steric attributes serve to block hydride transfer from $\mathbf{2}^{Np}$-H, thereby allowing complexation pathways to dominate.

An additional illustration of the early metal hydride character of $\mathbf{2}^{Np}$-H is obtained from its reactivity toward both carbon monoxide (CO) and isopropylisocyanide (*i*-PrNC). As shown in Scheme 10, treatment of $\mathbf{2}^{Np}$-H with carbon monoxide (CO) or isopropylisocyanide (*i*-PrNC) results in the clean formation of the enolate-imido and

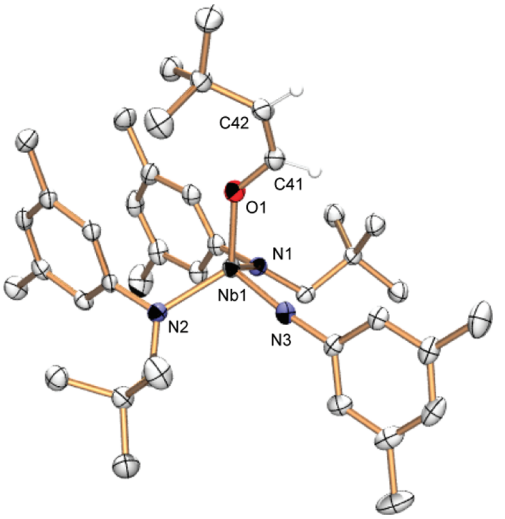

Figure 5. Molecular structure of complex **7**. Selected bond distances (Å) and angles (deg): Nb(1)−O(1) = 1.956(2); Nb(1)−N(3) = 1.762(3); Nb(1)−N(2) = 1.996(3); C(41)−C(42) = 1.321(5); Nb(1)−N(3)−C(31) = 174.3(3).

Scheme 10

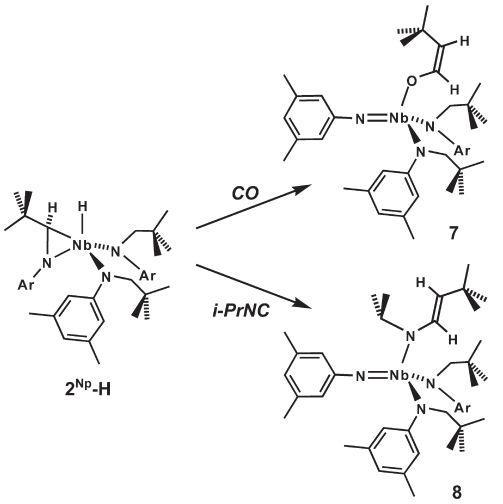

eneamido-imido complexes **7** and **8**, respectively. Crystallographic characterization of **7** and **8** (Figures 5 and 6, respectively) revealed that a neopentylidene group is incorporated into the newly formed olefinic fragments, demonstrating that both CO and *i*-PrNC induce the cleavage of the *N*-C*H*(*t*-Bu) linkage of the N[Np]Ar ligand. Furthermore, in both **7** and **8**, an H atom is delivered to the terminal carbon atom of the incoming substrate. Therefore, we suggest that the formation of complexes **7** and **8** arises from rapid insertion of CO or *i*-PrNC into the Nb−H unit in $\mathbf{2}^{Np}$-H, concomitant with the formation of an incipient formyl[91−94] or iminoformyl[95,96] ligand, respectively. The latter subsequently

(90) Espenson, J. H. *Chemical Kinetics and Reaction Mechanisms*, 2nd ed.; McGraw-Hill: New York, 2002; pp 58−61.

(91) Wolczanski, P. T.; Bercaw, J. E. *Acc. Chem. Res.* **1980**, *13*, 121–127.
(92) Fagan, P. J.; Moloy, K. G.; Marks, T. J. *J. Am. Chem. Soc.* **1981**, *103*, 6959–6962.
(93) Gladysz, J. A. *Adv. Organomet. Chem.* **1982**, *20*, 1–38.
(94) Reinartz, S.; Brookhart, M.; Templeton, J. L. *Organometallics* **2002**, *21*, 247–249, and references therein.
(95) Durfee, L. D.; Rothwell, I. P. *Chem. Rev.* **1988**, *88*, 1059–1079.
(96) Clark, J. R.; Fanwick, P. E.; Rothwell, I. P. *Organometallics* **1996**, *15*, 3232–3237.

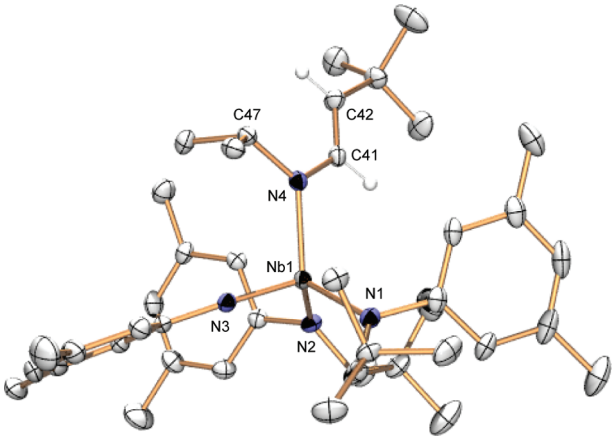

Figure 6. Molecular structure of complex **8**. Selected bond distances (Å) and angles (deg): Nb(1)−N(3) = 1.760(3); Nb(1)−N(4) = 2.037(3); Nb(1)−N(1) = 1.997(3); Nb(1)−N(2) = 2.030(3); N(4)−C(41) = 1.400(4); C(41)−C(42) = 1.336(5); Nb(1)−N(3)−C(31) = 170.9(2).

succumbs to nucleophilic attack[96,97] by the niobaziridine carbon atom to furnish the observed products after electronic rearrangement and C−N bond cleavage.

Proposed Mechanism of Reaction of Niobaziridine Hydride 2^{Np}-H with Small Molecules. Both the isotopic labeling studies and reaction chemistry described above offer insight into the elementary steps by which niobaziridine hydride 2^{Np}-H interacts with incoming substrates. The inverse isotope effect observed for the decomposition of 2^{Np}-H and 2^{Np}-D strongly indicates that rapid interconversion between three-coordinate 1^{Np} and 2^{Np}-H occurs in solution. However, 1^{Np} is exceedingly reactive and likely not present in appreciable concentration in which to interact with substrate. Therefore the direct reaction of substrates with 1^{Np} likely does not take place (Scheme 11, pathway A). Instead, we suggest that substrates first associatively bind to five-coordinate 2^{Np}-H to form a six-coordinate substrate→2^{Np}-H species (pathway B). This mechanism is inferred from the finding that unsaturated substrates readily succumb to migratory hydride transfer as described above (pathway C). Indeed, insertion into the M−H bond of early metal hydrides is well known to involve a requisite substrate binding event,[98] which precedes migratory hydride transfer. While a substrate→2^{Np}-H species has not been observed spectroscopically by us to date, evidence for such intermediates has been obtained previously for other early metal hydrides.[91,99−101]

Importantly, on the basis of stopped-flow kinetic measurements and isotopic labeling studies, an analogous associative mechanism has also been proposed for the reaction between molybdaziridine hydride $3^{i\text{-}Pr}$-H and isocyanides (RNC). In this latter case, insertion chemistry is *not* observed. Instead, binding of RNC to $3^{i\text{-}Pr}$-H promotes coordinatively induced C−H reductive elimination[102−106] and access to the Mo(N[*i*-Pr]Ar)$_3$ fragment. Accordingly, it is suggested that the complexation and atom abstraction chemistry observed by 2^{Np}-H is also the result of coordinatively induced C−H reductive elimination, but is only manifest with substrates for which insertion is inhibited. Thus for MesCN, substitution at both *ortho* positions apparently serves to protect its CN unit from hydride transfer, thereby allowing for C−H reductive elimination and subsequent complexation to the 1^{Np} fragment. Contrastingly, PhCN readily undergoes insertion due to the unprotected nature of its CN unit. For the intermediate case of *o*-tolCN, a partial inhibition of hydride transfer is postulated to be operative, where insertion vs complexation chemistry is dictated by the spatial presentation of the single *ortho*-Me group to the Nb−H unit in 2^{Np}-H.[107]

Associative binding followed by C−H reductive elimination is also likely operative in the deoxygenation of $OPPh_3$ by 2^{Np}-H, since, to our knowledge, hydrogenation of phosphine oxides by transition metal hydrides is unprecedented. This fact, coupled with the demonstrated need for a powerful reductant to effect phosphoryl P=O bond cleavage,[75−77] further adds to the suggestion that the reactive, d^2 1^{Np} fragment becomes available upon the addition of $OPPh_3$ to 2^{Np}-H. However, O=PPh_3 hydrogenation is not completely precluded by the present set of data. Accordingly, whereas coordinatively induced reductive elimination may account for the formation of the heavier chalcogenido complexes 1^{Np}-E (E = S, Se, Te), direct chalcogen-atom insertion into the Nb−H bond of 2^{Np}-H, followed by α-H abstraction by the niobaziridine ring, also cannot be ruled out at present. Indeed, α-H abstraction of hydrochalcogenido ligands (M−EH) has been proposed as a likely mechanistic pathway for the formation of heavier terminal chalcogenido functionalities (M=E; E = S, Se, Te).[73]

Additional Niobaziridine Hydride Variants. Synthesis and Thermal Behavior of Niobaziridine Hydrides Derived from *N*-Methylene-1-adamantyl (*N*-CH_2-^{1}Ad) and *N*-Cyclohexyl (*N*-*cyclo*-C_6H_{11}) Anilides. Due to the rich chemistry displayed by 2^{Np}-H, we became interested in expanding the library of kinetically persistent niobaziridine hydrides. To this end, we targeted for synthesis niobaziridine hydrides derived from both *N*-methylene-1-adamantylanilide (N[$CH_2{}^1$Ad]Ar) and *N*-cyclohexylanilide (N[Cy]Ar, Cy = *cyclo*-C_6H_{11}), hoping that stable niobaziridine hydrides would be generally obtainable by judicious choice of ancillary ligand. The decision to employ N[$CH_2{}^1$Ad]Ar as a variant was based on its structural similarity to the N[Np]Ar ligand. In addition, we thought the relatively encumbering N[Cy]Ar ligand may provide a room-temperature-stable niobaziridine hydride featuring a secondary hydrocarbyl substituent, whereas the N[*i*-Pr]Ar ligand failed in that regard.

Gratifyingly, Mg(THF)$_3$(anthracene) reduction of the diiodide precursors 1^{CH_2Ad}-I_2 and 1^{Cy}-I_2 readily provided the niobaziridine hydrides Nb(H)(η^2-^{1}Ad(H)C=NAr)(N[$CH_2{}^1$Ad]-Ar)$_2$ (2^{CH_2Ad}-H) and Nb(H)(η^2-C_5H_{10}C=NAr)(N[Cy]Ar)$_2$ (2^{Cy}-H), respectively (Scheme 12). Complexes 2^{CH_2Ad}-H and

(97) For a proposed nucleophilic attack on an incipient formyl ligand, see: Fryzuk, M. D.; Mylvaganam, M.; Zaworotko, M. J.; MacGillivray, L. R. *Organometallics* **1996**, *15*, 1134–1138.
(98) For early examples, see: (a) Fachentti, G.; Floriani, C. *J. Organomet. Chem.* **1974**, *71*, C5–C7. (b) Röder, A.; Thiele, K.-H.; Pályi, G.; Markó, L. *J. Organomet. Chem.* **1980**, *199*, C31–C34.
(99) Manriquez, J. M.; McAlister, D. R.; Sanner, R. D.; Bercaw, J. E. *J. Am. Chem. Soc.* **1978**, *100*, 2716–2724.
(100) Marsella, J. A.; Curtis, C. J.; Bercaw, J. E.; Caulton, K. G. *J. Am. Chem. Soc.* **1980**, *102*, 7244–7246.
(101) Burger, B. J.; Santarsiero, B. D.; Trimmer, M. S.; Bercaw, J. E. *J. Am. Chem. Soc.* **1988**, *110*, 3134–3146.
(102) Yoshifuji, M.; Gell, K. I.; Schwartz, J. *J. Organomet. Chem.* **1978**, *153*, C15–C18.
(103) Gell, K. I.; Schwartz, J. *J. Am. Chem. Soc.* **1981**, *103*, 2687–2695.
(104) Gell, K. I.; Schwartz, J. *J. Organomet. Chem.* **1978**, *162*, C11–C15.
(105) Jones, W. D.; Hessell, E. T. *J. Am. Chem. Soc.* **1992**, *114*, 6087–6095.
(106) Burkey, D. J.; Debad, J. D.; Legzdins, P. *J. Am. Chem. Soc.* **1997**, *119*, 1139–1140.
(107) The observed product ratio of 2^{Np}-NC(H)*o*-tol:1^{Np}-NC-*o*-tol may be a manifestation of the rate of rotation about of the aryl unit about the C_{ipso}−$C_{nitrile}$ bond.

Scheme 11

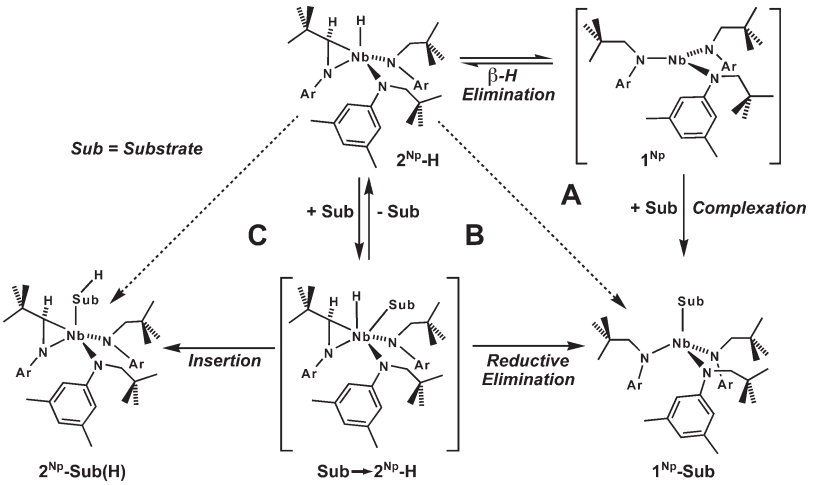

Scheme 12

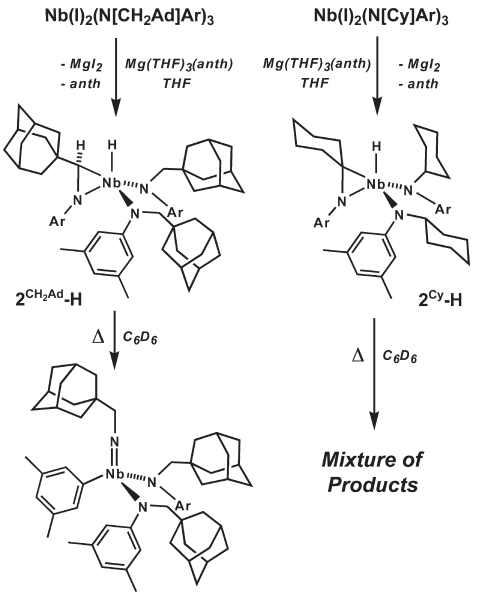

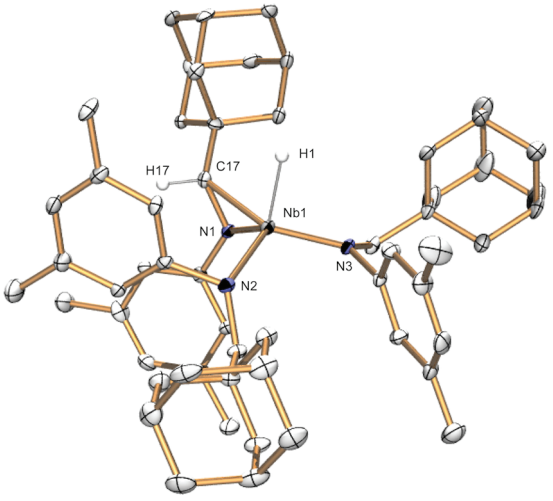

Figure 7. Molecular structure of $\mathbf{2}^{CH_2Ad}$-H. Selected bond distances (Å) for one of two independent molecules: Nb(1)−N(1) = 1.994(6); Nb(1)−C(17) = 2.209(7); Nb(1)−N(2) = 1.973(6); Nb(1)−N(3) = 1.992(6); C(17)−N(1) = 1.415(8); C(11)−N(1) = 1.396(9).

$\mathbf{2}^{Cy}$-H are characterized by broad ^{1}H NMR resonances centered at 9.34 and 9.50 ppm, respectively, which are attributed to their Nb-*H* units and are comparable with that of $\mathbf{2}^{Np}$-H (9.24 ppm). While $\mathbf{2}^{Cy}$-H has not been structurally characterized in the solid state, X-ray diffraction revealed that $\mathbf{2}^{CH_2Ad}$-H is a monomer in the solid state and possesses overall features similar to $\mathbf{2}^{Np}$-H (Figure 7). Moreover, both $\mathbf{2}^{Cy}$-H and $\mathbf{2}^{CH_2Ad}$-H insert benzaldehyde to give the alkoxy products $\mathbf{2}^{R}$-OCH_2Ph, and $\mathbf{2}^{CH_2Ad}$-H will deoxygenate N_2O to afford ONb-$(N[CH_2{}^1Ad]Ar)_3$ ($\mathbf{1}^{CH_2Ad}$-O).

With respect to their thermal behavior in solution, both $\mathbf{2}^{CH_2Ad}$-H and $\mathbf{2}^{Cy}$-H are indeed stable at room temperature for extended periods. When heated in C_6D_6, niobaziridine hydride $\mathbf{2}^{CH_2Ad}$-H smoothly converts to its aryl-imido isomer, as indicated by ^{1}H NMR spectroscopy, thus confirming its similarity to $\mathbf{2}^{Np}$-H (Scheme 12).[108] Contrastingly, cyclohexyl-substituted $\mathbf{2}^{Cy}$-H does not exhibit clean decomposition behavior at elevated temperatures. Instead, a myriad of resonances appear when $\mathbf{2}^{Cy}$-H is heated at 65 °C, as assayed by ^{1}H NMR spectroscopy (C_6D_6). Such decomposition behavior is reminiscent of the *i*-Pr derivative $\mathbf{2}^{i\text{-}Pr}$-H, presumably indicating that anilido ligands featuring a secondary hydrocarbyl substituent do not effectively direct niobaziridine hydride decomposition in a clean unimolecular fashion.

Reinvestigation of Dicyclohexyl Amido-Derived (NCy_2) Niobaziridine Systems. To date, we have not obtained evidence for the ability of complex $\mathbf{2}^{Np}$-H alone to engage in dinitrogen activation chemistry.[109] Indeed, $\mathbf{2}^{Np}$-H does not react with N_2 at room temperature or below, or at N_2 pressures ranging from 1 to 4 atm.[110] In addition, niobaziridine hydrides $\mathbf{2}^{i\text{-}Pr}$-H, $\mathbf{2}^{CH_2Ad}$-H, and $\mathbf{2}^{Cy}$-H are similarly unreactive toward N_2 under ambient conditions.

(108) Under similar thermolysis conditions, niobaziridine hydride $\mathbf{2}^{CH_2Ad}$ has been qualitatively observed to decompose faster than the neopentyl variant $\mathbf{2}^{Np}$-H. We tentatively ascribe this relative difference to added steric pressures in $\mathbf{2}^{CH_2Ad}$-H as induced by the pendent 1-Ad substituents.

(109) In previous work, we employed dinitrogen anions of molybdenum for the delivery of N_2 to the $\mathbf{1}^{Np}$ fragment. That work was independent of niobaziridine hydride $\mathbf{2}^{Np}$-H. See ref 29.

(110) We have also investigated the treatment of $\mathbf{2}^{Np}$-H with Lewis basic additives in order to promote niobaziridine hydride opening and subsequent N_2 binding. However such experiments, where excesses of [2.2.2]-diazabicyclooctane (DABCO) or PMe_3 were added to solutions of $\mathbf{2}^{Np}$-H, failed to elicit N_2 activation. In addition, neither DABCO nor PMe_3 was observed to bind to $\mathbf{2}^{Np}$-H on the ^{1}H NMR time scale.

Scheme 13

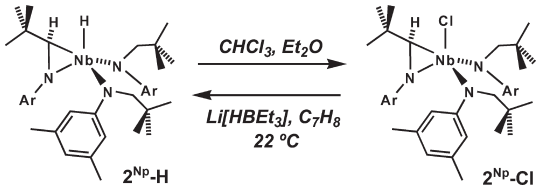

Scheme 14

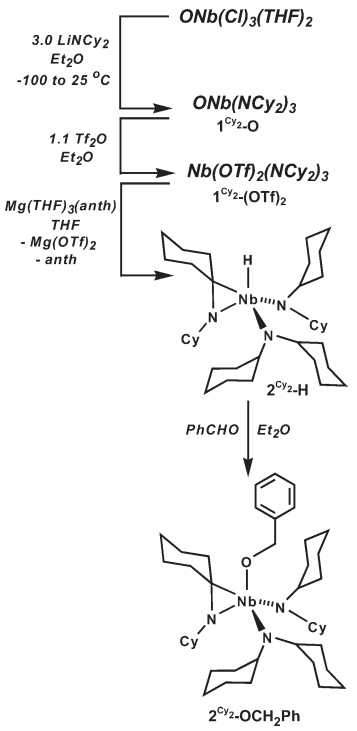

This lack of N_2 reactivity is surprising given the ability of the NCy_2-ligated niobaziridine chloride complex of Berno and Gambarotta to activate N_2 upon the addition of $Na[HBEt_3]$.[45] Notably, a niobaziridine chloride complex of our N[Np]Ar system is readily available from the reaction between $\mathbf{2}^{Np}$-H and $CHCl_3$ or CH_2Cl_2 ($\mathbf{2}^{Np}$-Cl, Scheme 13). However, treatment of $\mathbf{2}^{Np}$-Cl with $Li[HBEt_3]$ in toluene in the presence of N_2, conditions which closely mimic those employed for the NCy_2/Nb system, results exclusively in the regeneration of $\mathbf{2}^{Np}$-H.

Therefore, on the basis of the possibility that the niobaziridine hydride Nb(H)(*cyclo*-$C_5H_{10}C{=}NCy)(NCy_2)_2$ ($\mathbf{2}^{Cy_2}$-H) is an intermediate en route to N_2 complexation in the NCy_2-ligated system, we sought its isolation in pure form in order to compare its behavior with that of our anilido-derived complexes.

A multistep synthetic strategy provided niobaziridine hydride $\mathbf{2}^{Cy_2}$-H, thus confirming that it is indeed amenable to isolation (Scheme 14). As revealed by X-ray diffraction (Figure 8), the complement of cyclohexyl units provides adequate protection to engender a monomeric niobaziridine hydride in the solid state. However, the Nb center in $\mathbf{2}^{Cy_2}$-H is found to possess intramolecular H−C agostic interactions[69,70] from two intact NCy_2 ligands (2.466 Å av). Close $H_{Cy}{\rightarrow}$Nb contacts are also observed in the solid-state structure of Nb(Cl)(*cyclo*-$C_5H_{10}C{=}NCy)(NCy_2)_2$ ($\mathbf{2}^{Cy_2}$-Cl), but were attributed to arise from steric

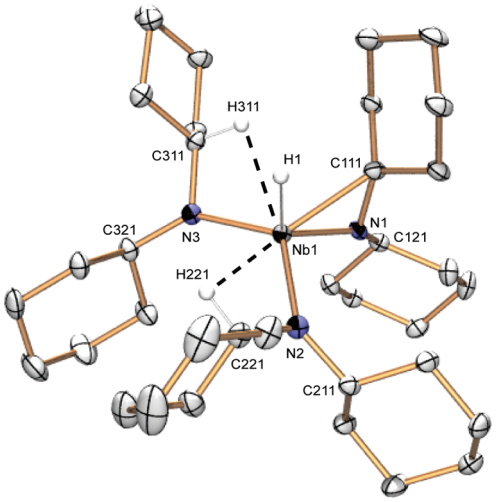

Figure 8. Molecular structure of $\mathbf{2}^{Cy_2}$-H. Selected bond distances (Å): Nb(1)−H(1) = 1.818(10); Nb(1)−N(1) = 1.959(2); Nb(1)−C(111) = 2.231(3); Nb(1)−N(2) = 1.986(2); Nb(1)−N(3) = 1.986(2); N(1)−C(111) = 1.425(3); N(1)−C(121) = 1.467(3); Nb(1)···H(221) = 2.492; Nb(1)···H(311) = 2.441.

pressures of the encumbering Cy substituents.[45] On the basis of the structures of both dimer $[\mathbf{2}^{i\text{-}Pr}\text{-H}]_2$ and monomer $\mathbf{2}^{Np}$-H however, we suggest that the $H_{Cy}{\rightarrow}$Nb contacts in $\mathbf{2}^{Cy_2}$-H and $\mathbf{2}^{Cy_2}$-Cl result from the presence of highly Lewis acidic Nb centers, which agostic interactions serve to stabilize. To this end $\mathbf{2}^{Cy_2}$-H, like $\mathbf{2}^{Np}$-H, has been found to function as a Lewis acidic hydride complex as demonstrated by the facile insertion of benzaldehyde into its Nb−H bond (Scheme 14, $\mathbf{2}^{Cy_2}$-OCH_2Ph).[111]

Most interestingly, niobaziridine hydride $\mathbf{2}^{Cy_2}$-H is stable for extended periods in common organic solvents, but does not form the bridging dinitrogen complex $(\mu_2\text{-}N_2)[Nb(NCy_2)_3]_2$ when exposed to N_2. Furthermore, to date, we have not identified suitable conditions under which $\mathbf{2}^{Cy_2}$-H will elicit N_2 activation chemistry. Thus we contend that the electronic and steric differences attendant in dicyclohexylamido vs *N*-hydrocarbylanilido ligation do not affect the ability of the niobaziridine hydride functionality to interact with dinitrogen under ambient conditions. Accordingly, the factors governing the ability of $\mathbf{2}^{Cy_2}$-Cl to activate N_2 in the presence of $NaHBEt_3$, as reported by Berno and Gambarotta, remain unclear.

Niobaziridine Hydride Radical Anion and Comparison of Nioba- and Molybdaziridine Hydride Complexes. Despite their shared characteristics, the fact that insertion chemistry is prominent for niobaziridine hydride $\mathbf{2}^{Np}$-H but nonexistent for molybdaziridine hydride $\mathbf{3}^{i\text{-}Pr}$-H is particularly striking. Furthermore, the ability of molybdaziridine hydride $\mathbf{3}^{i\text{-}Pr}$-H to cleave dinitrogen, whereas niobaziridine hydrides $\mathbf{2}^{R}$-H do not react with N_2, highlights another major dichotomy between these Mo- and Nb-based systems. While the greater electronegativity of Mo relative to Nb may impede the hydride in $\mathbf{3}^{i\text{-}Pr}$-H from serving as a nucleophile,[112] such an argument falters given that several

(111) Complex $\mathbf{2}^{Cy_2}$-OCH_2Ph has been formulated on the basis of its ^{1}H NMR spectroscopic signatures, which indicate three distinct cyclohexyl environments and OCH_2Ph ligand resonances similar to those in complex $\mathbf{2}^{Np}$-OCH_2Ph. For details, see the Supporting Information.

(112) Labinger, J. A.; Bercaw, J. E. *Organometallics* **1988**, *7*, 926–928.

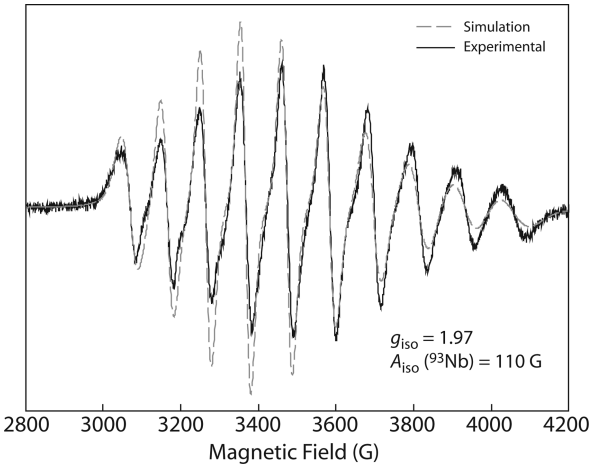

Figure 9. X-band EPR spectrum of K[$\mathbf{2}^{Np}$-H] in THF at 20 °C.

Scheme 15

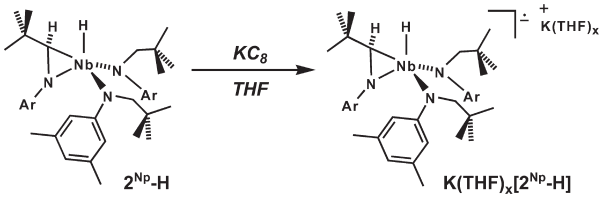

mononuclear Mo-hydride species are known to insert unsaturated substrates.[113−117] Therefore, we were intrigued at the possibility that the differing *d*-electron count between complexes $\mathbf{3}^{i\text{-Pr}}$-H and $\mathbf{2}^{Np}$-H (Mo(V), d^1 vs Nb(V), d^0) may ultimately be responsible for modulating the disparate reactivity of these metallaziridine hydride complexes. To test this hypothesis, we sought the radical anion of $\mathbf{2}^{Np}$-H as an isoelectronic surrogate to molybdaziridine hydride $\mathbf{3}^{i\text{-Pr}}$-H on the basis that it may likewise be resistant to insertion chemistry.

Synthetic access to a radical anion appeared feasible based on cyclic voltammetry measurements on $\mathbf{2}^{Np}$-H, which revealed a clean and reversible reduction wave centered at −2.7 V (vs Fc/Fc^+, 0.2 M ^{n}Bu$_4$NPF$_6$/THF).[118] Accordingly, addition of KC_8[57] to $\mathbf{2}^{Np}$-H in THF rapidly induced a color change from orange to forest green. Analysis of this solution by EPR spectroscopy revealed a 10-line spectral pattern (ca. 1000 G, Figure 9), indicative of a paramagnetic, formally Nb^{IV} species (^{93}Nb, I = 9/2 100%).[55,119,120] Whereas we attribute this spectroscopic signature to the radical species K[$\mathbf{2}^{Np}$-H] (Scheme 15), its isolation as generated from KC_8 proved difficult. Indeed, while the green color of presumed K[$\mathbf{2}^{Np}$-H] persists at −35 °C in THF, warming to room temperature induced a color change to brown and the formation of an intractable mixture of products (ca. 1 h), as indicated by both ^{1}H NMR and EPR spectroscopic measurements.

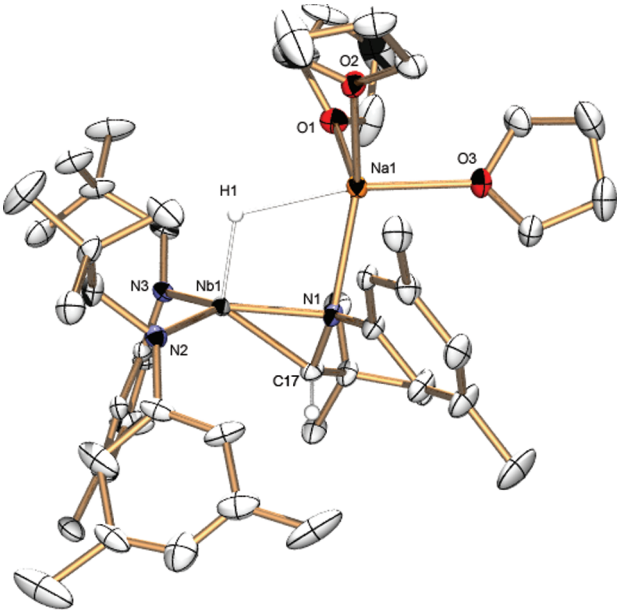

Figure 10. Molecular structure of Na(THF)$_3$[$\mathbf{2}^{Np}$-H]. Selected bond distances (Å): Nb(1)−H(1) = 1.76(4); Nb(1)−N(1) = 2.113(3); Nb(1)−C(17) = 2.187(4); Nb(1)−N(2) = 2.092(3); Nb(1)−N(3) = 2.022(3); C(17)−N(1) = 1.434(4); C(11)−N(1) = 1.400(5); H(1)−Na(1) = 2.36(4); N(1)−Na(1) = 2.474(3).

Fortuitously however, during a Na/Hg reduction of the bis-triflate complex $\mathbf{2}^{Np}$-(OTf)$_2$, we obtained a small amount of a dark green, *n*-pentane-insoluble material[121] that proved amenable to crystallization from THF. X-ray diffraction established the identity of this material as the [Na(THF)$_3$] salt of the [$\mathbf{2}^{Np}$-H]$^-$ radical anion (Figure 10), thereby confirming the latter's accessibility via chemical reduction. Furthermore, dissolution of crystalline [Na(THF)$_3$][$\mathbf{2}^{Np}$-H] in THF followed by EPR spectroscopic analysis gave rise to the identical spectral signature obtained upon reduction of $\mathbf{2}^{Np}$-H with KC_8. Unfortunately, repeated attempts to isolate [Na(THF)$_3$][$\mathbf{2}^{Np}$-H] from the $\mathbf{2}^{Np}$-(OTf)$_2$/Na/Hg reaction system led to inconsistent results. However, due to the EPR spectral similarities between [Na(THF)$_3$][$\mathbf{2}^{Np}$-H] and presumed K[$\mathbf{2}^{Np}$-H], we felt confident that *in situ* generation of the latter would serve adequately for synthetic investigations.

While stable in solution at −35 °C, K[$\mathbf{2}^{Np}$-H] does not react with N_2, as indicated by ^{1}H NMR spectroscopy. This finding contrasts with the behavior of d^1 molybdaziridine hydride $\mathbf{3}^{i\text{-Pr}}$-H, which effects N_2 cleavage at low temperature in solution en route to the bridging nitrido species (μ-N)-[Mo(N[*i*-Pr]Ar)$_3$]$_2$.[39,41] Addition of Lewis basic additives, which are known to promote and accelerate the overall N_2 cleavage reaction by $\mathbf{3}^{i\text{-Pr}}$-H,[41] had no effect on the integrity of K[$\mathbf{2}^{Np}$-H]. Furthermore, treatment of K[$\mathbf{2}^{Np}$-H] with PhCN rapidly generated the ketimido species $\mathbf{2}^{Np}$-NC(H)Ph according to ^{1}H NMR analysis, presumably generating K^0 as a byproduct. Notably, molybdaziridine hydride $\mathbf{3}^{i\text{-Pr}}$-H is competent for both the coupling and C≡N cleavage of

(113) Kubas, G. J.; Wasserman, H. J.; Ryan, R. R. *Organometallics* **1985**, *4*, 2012–2021.
(114) Ito, T.; Igarashi, T. *Organometallics* **1987**, *6*, 199–201.
(115) Liang, F. P.; Jacobsen, H.; Schmalle, H. W.; Fox, T.; Berke, H. *Organometallics* **2000**, *19*, 1950–1962.
(116) Liang, F.; Schmalle, H. W.; Fox, T.; Berke, H. *Organometallics* **2003**, *22*, 3382–3393.
(117) Liang, F.; Schmalle, H. W.; Berke, H. *Inorg. Chem.* **2004**, *43*, 993–999.
(118) Such a negative reduction potential is within the range attainable by strong chemical reductants; see: Connelly, N. G.; Geiger, W. E. *Chem. Rev.* **1996**, *96*, 877–910.
(119) Cotton, F. A.; Lu, J. *Inorg. Chem.* **1995**, *34*, 2639–2644.
(120) Sanchez, C.; Vivien, D.; Livage, J.; Sala-Pala, J.; Viard, B.; Guerchais, J.-E. *J. Chem. Soc., Dalton Trans.* **1981**, 64–68.

(121) The major product of this reduction experiment was niobaziridine hydride $\mathbf{2}^{Np}$-H.

PhCN without displaying insertion reactivity.[39,42] Thus for N_2 and PhCN, the [$\mathbf{2}^{Np}$-H]$^-$ fragment behaves similarly to neutral $\mathbf{2}^{Np}$-H, rather than d^1 $\mathbf{3}^{i\text{-}Pr}$-H, despite the presence of added electron density.

Conclusions

The niobaziridine hydride functional group has been characterized for several ligand variants. In doing so, the divergent reactivity of these complexes—insertion reactions vs retrocyclometalation—has been explored. We have proposed two possible mechanisms for the observed reactivity: rapid reversible β-hydride elimination to interconvert three-coordinate, d^2 $\mathbf{1}^{Np}$ with $\mathbf{2}^{R}$-H or competing coordinatively induced reductive elimination and insertion from an intermediate [Substrate·$\mathbf{2}^{R}$-H] complex. The latter reactivity is consistent with the high degree of Lewis acidity that these complexes display. One aspect of this Lewis acidity is revealed in the decomposition pathways of $\mathbf{2}^{R}$-H and the need for sufficient steric protection to render them kinetically stable for isolation. Despite efforts to probe the possible role of niobaziridine hydrides in N_2 activation chemistry, to date they have not been shown to be capable of N_2 binding with either d^0 or d^1 electron configurations. In any case, a rich chemistry of the niobaziridine hydride functional group has been elucidated, but by no means has this area been exhaustively explored.

Experimental Section

General Procedures. All manipulations were carried out at room temperature, under an atmosphere of purified dinitrogen, using a Vacuum Atmospheres glovebox or Schlenk techniques. All solvents were obtained anhydrous and oxygen-free according to standard purification procedures. Benzene-d_6 (C_6D_6) and toluene-d_8 (C_7D_8) were degassed and stored in the glovebox over 4 Å molecular sieves for at least 3 d prior to use. Celite 435 (EM Science) and 4 Å molecular sieves (Aldrich) were dried under vacuum at 250 °C overnight and stored under dinitrogen. Benzaldehyde and *tert*-butylnitrile were purchased from Aldrich and distilled from CaH_2 prior to use. 2,4,6-Trimethylbenzonitrile (MesCN, Aldrich) was recrystallized from *n*-hexane and dried *in vacuo* prior to use. Nitrous oxide (N_2O) was obtained from BOC Gases and passed through a 1 ft column of P_2O_5 before being introduced to the reaction vessel via a Schlenk line. The compounds $Mg(THF)_3$(anthracene),[58] *mer,cis*-$NbCl_3(THF)_2$(PhCCPh),[122] and Ph_2CN_2[123] were prepared according to literature procedures. Complexes $\mathbf{2}^{Np}$-H, $\mathbf{5}^{Np}$, $\mathbf{2}^{Np}$-NCMes, $\mathbf{2}^{Np}$-NC(H)*t*-Bu, and $\mathbf{2}^{Np}$-OBz were prepared as previously reported unless otherwise stated.[34] Complexes $\mathbf{1}^{R}$-I_2 and $\mathbf{1}^{R}$-PhCCPh were prepared according to the methods outlined for the $\mathbf{1}^{Np}$ system, and these procedures are detailed in the Supporting Information. For details concerning niobium complexes of the N(*t*-Bu)Ar ligand system, please see the Ph.D. Thesis of Michael G. Fickes.[123] All other reagents were obtained from commercial sources and used as received or purified according to standard procedures. All glassware was oven-dried at a temperature of 170 °C prior to use.

Synthesis of the Niobaziridine Hydride Complex Nb(H)(η^2-Me_2C=NAr)(N[*i*-Pr]Ar)$_2$ ($\mathbf{2}^{iPr}$-H) and (μ-NAr)(μ-N[*i*-Pr]C_6H_2-Me_2)Nb_2(N[*i*-Pr]Ar)$_4$ ($\mathbf{4}^{iPr}$). Complex $\mathbf{2}^{iPr}$-H was prepared analogously to complex $\mathbf{2}^{Np}$-H by employing 2.5 g (2.99 mmol) of $Nb(I)_2$(N[*i*-Pr]Ar)$_3$ ($\mathbf{2}^{iPr}$-I_2). It was found that the total reaction time including workup should be carried out on the order of 2.0 h to avoid decomposition of $\mathbf{2}^{iPr}$-H to the forest green dimeric species $\mathbf{4}^{iPr}$. Dark orange single crystals of $\mathbf{2}^{iPr}$-H were obtained from a saturated Et_2O solution stored at −35 °C for 1 d in approximately 30% yield (0.897 mmol). Complex $\mathbf{2}^{iPr}$-H was found to completely decompose over the course of 1 h to forest green $\mathbf{4}^{iPr}$ when heated at 65 °C and over the course of 4 h when left standing at room temperature (C_6D_6). Data for $\mathbf{2}^{iPr}$-H: ^{1}H NMR (300 MHz, C_6D_6, 23 °C): δ 9.23 (br s, 1H, Nb-*H*), 7.23 (s, 2H, *o*-Ar, aziridine), 7.15 (s, 1H, *p*-Ar, aziridine), 6.70 (s, 4H, *o*-Ar amido), 6.59 (s, 2H, *p*-Ar amido), 3.68 (septet, 2H, J = 4 Hz, C*H*$(CH_3)_2$), 2.37 (s, 6H, Ar-CH_3 aziridine), 2.07 (s, 12H, Ar-CH_3 amido), 2.02 (s, 6H, N=C(CH_3)$_2$ aziridine), 1.00 (d, 6H, J = 4 Hz, CH(CH_3)$_2$ amido), 0.96 (d, 6H, J = 4 Hz, CH(CH_3)$_2$ amido). The thermal instability of $\mathbf{1}^{iPr}$-H precluded a satisfactory combustion analysis. Data for $\mathbf{4}^{iPr}$: ^{1}H NMR (300 MHz, C_6D_6, 23 °C): δ 7.28 (s, *p*-Ar), 6.71 (s, *o*-Ar), 6.69 (s, *o*-Ar), 6.55 (s, *p*-Ar), 6.23 (s, *p*-Ar), 4.09 (br, C*H*$(CH_3)_2$), 3.57 (br, C*H*$(CH_3)_2$), 2.67 (s, ArCH_3), 2.45 (s, ArCH_3), 2.26 (s, ArCH_3), 2.18 (s, ArCH_3), 1.21 (br, CH(CH_3)), 0.99 (d, CH(CH_3)), 0.94 (d, CH(CH_3)). ^{13}C{^{1}H} NMR (75.0 MHz, C_6D_6, 23 °C): δ 168.6, 152.9, 139.7, 138.2, 137.9, 137.8, 128.9, 128.7, 128.0, 127.9, 125.8, 125.3, 118.7, 117.8, 66.27, 53.41, 52.44, 34.78, 27.64, 24.67, 23.84, 23.08, 22.41, 21.99, 21.76, 15.95, 14.64. IR (CaF_2, Et_2O): 2960 (m), 2933 (m), 2873 (m), 1998 (w), 1811 (w), 1596 (s), 1583 (s), 1375 (w), 1295 (w) 1170 (w) cm^{-1}. Anal. Calcd for $C_{63}H_{89}N_6Nb_2$: C, 67.79; H, 8.04; N, 7.53. Found: C, 67.64; H, 7.94; N, 7.42. Mp: 152−154 °C.

Synthesis of the Insertion Products $\mathbf{2}^{Np}$-NC(H)NMe_2, $\mathbf{2}^{Np}$-NC(H)=C(H)*t*-Bu, and $\mathbf{2}^{Np}$-N(H)$NCPh_2$. For each reaction, 0.100 g (0.150 mmol) of $\mathbf{2}^{Np}$-H was dissolved in 1.5 mL of C_6D_6. To this solution was added 1.05 equiv of the corresponding reagent (Me_2NCN, *t*-BuCCH, and Ph_2CN_2, respectively) dissolved in 0.5 mL of C_6D_6. The reactions were monitored by ^{1}H NMR ca. 30 min after mixing and were observed to be complete. Total reaction time for each was approximately 1.5 h. The reaction mixtures were evaporated to dryness, extracted with *n*-pentane, and filtered through Celite. For $\mathbf{2}^{Np}$-C(H)=C(H)*t*-Bu: Orange crystals from Et_2O (−35 °C, 3 d). Yield: 0.080 g, 0.107 mmol, 71% in two crops. ^{1}H NMR (300 MHz, C_6D_6, 23 °C): δ 8.19 (d, 1H, J = 18 Hz, C(*H*)=C(H)*t*-Bu), 7.31 (s, 2H, *o*-Ar), 6.98 (s, 2H, *o*-Ar), 6.62 (s, 1H, *p*-Ar), 6.58 (s, 1H, *p*-Ar), 6.55 (s, 1H, *p*-Ar), 6.41 (s, 2H, *o*-Ar), 6.36 (d, 1H, J = 18 Hz, C(H)=C(*H*)*t*-Bu), 4.26 (d, 1H, J = 14 Hz, N-CH_2), 4.16 (d, 1H, J = 14 Hz, N-CH_2), 2.87 (d, 1H, J = 14 Hz, N-CH_2), 2.75 (d, 1H, J = 14 Hz, N-CH_2), 2.60 (s, 1H, N=C(*H*)*t*-Bu aziridine), 2.37 (s, 6H, Ar-CH_3), 2.26 (s, 6H, Ar-CH_3), 2.15 (s, 6H, Ar-CH_3), 1.39 (s, 9H, *t*-Bu), 1.26 (s, 9H, *t*-Bu), 0.83 (s, 9H, *t*-Bu), 0.45 (s, 9H, *t*-Bu). Anal. Calcd for $C_{45}H_{70}N_3Nb$: C, 72.45; H, 9.46; N, 5.63. Found: C, 71.93; H, 9.28; N, 5.89. Isolation procedures and characterization data for $\mathbf{2}^{Np}$-NC(H)-NMe_2 and $\mathbf{2}^{Np}$-N(H)$NCPh_2$ are provided in the Supporting Information.

Synthesis of the Cyclic Imido Complex Nb(=NC(H)*t*-BuC(H)*t*-BuNAr)(N[Np]Ar)$_2$ ($\mathbf{6}^{Np}$-*t*-Bu). A toluene solution of complex $\mathbf{2}^{Np}$-NC(H)*t*-Bu (0.150 g, 0.200 mmol, 3 mL) was heated at 120 °C for 1.5 h. A gradual color change from blood red to bright yellow was observed over this time. The toluene solvent was removed under reduced pressure, and the resulting yellow residue was extracted with *n*-pentane and filtered through Celite. The solvent was removed again, and the crude solid obtained was dissolved in approximately 0.5 mL of Et_2O. Yellow plates of **6a**-*t*-Bu were obtained from this solution upon standing at −35 °C for 3 d. Yield: 0.097 g, 0.130 mmol, 65% in two crops. ^{1}H NMR (400 MHz, C_6D_6, 23 °C): δ 7.02 (s, 2H, *o*-Ar), 6.95 (s, 2H, *o*-Ar), 6.56 (s, 1H, *p*-Ar), 6.49 (s, 1H, *p*-Ar), 6.35 (s, 1H, *p*-Ar), 6.05 (s, 2H, *o*-Ar), 5.29 (s, 1H, backbone), 4.68 (d, 1H, J = 13.4 Hz, N-CH_2), 4.29 (d, 1H, J = 13.4 Hz, N-CH_2), 4.14 (s, 1H, backbone), 3.94 (d, 1H, J=14 Hz, N-CH_2), 3.38 (d, 1H, J = 14 Hz, N-CH_2), 2.18 (s, 6H, Ar-CH_3), 2.14 (s, 6H, Ar-CH_3), 1.99 (s, 6H, Ar-CH_3), 1.26 (s, 9H, *t*-Bu), 1.14 (s, 9H, *t*-Bu), 0.99 (s, 9H, *t*-Bu), 0.84 (s, 9H, *t*-Bu). Anal. Calcd

(122) Hartung, J. B.; Pedersen, S. F. *Organometallics* **1990**, *9*, 1414–1417.

(123) Fickes, M. G. Ph.D. Thesis, Department of Chemistry, Massachusetts Institute of Technology, Cambridge, MA, 1998.

for $C_{44}H_{69}N_4Nb$: C, 70.75; H, 9.31; N, 7.50. Found: C, 69.94; H, 9.24; N, 7.30.

Reaction of 1a-H with CO. Synthesis of the Enolate Imido Complex Nb(OC(H)=C(H)*t*-Bu)(NAr)(N[Np]Ar)$_2$ (7). An excess of $CO_{(g)}$ was introduced to an Et_2O solution of $\mathbf{2}^{Np}$-H (0.100 g, 0.150 mmol, 3 mL), eliciting a rapid color change from orange to pale brown. The reaction mixture was allowed to stir for 1 h, at which point all volatile materials were removed *in vacuo*. The resulting pale yellow residue was extracted with *n*-pentane and filtered through Celite. The solvent was removed again, and the crude solid obtained was dissolved in approximately 0.5 mL of Et_2O. Yellow plates of **7** were obtained from this solution upon standing at −35 °C for several days. Yield: 0.046 g, 0.067 mmol, 45%. ^{1}H NMR (400 MHz, C_6D_6, 23 °C): δ 7.29 (d, 1H, J = 6.6 Hz, enolate), 6.98 (s, 2H, *p*-Ar amido), 6.70 (s, 4H, *o*-Ar amido), 6.52 (s, 1H, *p*-Ar imido), 6.36 (s, 1H, *o*-Ar, imido), 4.45 (d, 1H, J = 6.6 Hz, enolate), 4.45 (d, 2H, J = 13 Hz, N-CH_2), 3.83 (d, 2H, J = 13 Hz, N-CH_2), 2.11 (s, 6H, Ar-CH_3 amido), 2.10 (s, 12H, Ar-CH_3 imido), 1.47 (s, 9H, *t*-Bu enolate), 0.89 (s, 18H, *t*-Bu amido). ^{13}C{^{1}H} NMR (75.0 MHz, C_6D_6, 23 °C): δ 150.2 (aryl *ipso* amido), 149.2 (aryl *ipso* imido), 139.6 (*o*-Ar amido), 138.5 (*o*-Ar imido), 126.6 (*p*-Ar imido), 126.0 (*p*-Ar amido), 123.3 (*m*-Ar imido), 120.8 (*m*-Ar amido), 117.6 (enolate), 111.8 (enolate), 72.5 (N-*C*H2), 35.6 (*C*(CH$_3$)$_3$ anilide), 32.2 (*C*(CH$_3$)$_3$ enolate), 31.8 (C(*C*H$_3$)$_3$ enolate), 28.7 (C(*C*H$_3$)$_3$ amido), 21.9 (Ar-*C*H$_3$ amido), 21.6 (Ar-*C*H$_3$ imido). FT-IR (KBr windows, C_6D_6 solution): 2953, 2903, 1634, 1584, 1476, 1213, 1080, 686 cm^{-1}. Anal. Calcd for $C_{40}H_{60}N_3ONb$: C, 69.44; H, 8.74; N, 6.07. Found: C, 68.34; H, 8.56; N, 5.93.

Synthesis of the Niobaziridine Hydride Complex Nb(H)(η^2-Ad-(H)C=NAr)(N[CH$_2$-1-Ad]Ar)$_2$ ($\mathbf{2}^{CH_2Ad}$-H). Complex $\mathbf{2}^{CH_2Ad}$-H was prepared analogously to complex $\mathbf{2}^{Np}$-H employing 1.00 g (0.868 mmol) of $\mathbf{1}^{CH_2Ad}$-I$_2$ and 0.454 g (1.085 mmol, 1.25 equiv) of Mg(THF)$_3$(anthracene).[34] No special handling or attention to reaction time is required. Crude $\mathbf{2}^{CH_2Ad}$-H was extracted from MgI_2 and anthracene with Et_2O due to its low solubility in *n*-pentane. The cold-filtration step was performed using Et_2O; however some anthracene remained in the sample as assayed by ^{1}H NMR. To remove the residual anthracene, crude $\mathbf{2}^{CH_2Ad}$-H was dissolved in ca. 6 mL of Et_2O and left to stand overnight at −35 °C, whereupon the residual anthracene crystallized out. Concentration of the mother liquor to approximately 4 mL, followed by storage at −35 °C, afforded pure $\mathbf{2}^{CH_2Ad}$-H as a bright orange microcrystalline solid. Orange single crystals of $\mathbf{2}^{CH_2Ad}$-H were obtained from a dilute Et_2O solution left to stand at −35 °C for several weeks. Yield: 0.428 g, 0.477 mmol, 55%. ^{1}H NMR (300 MHz, C_6D_6, 23 °C): δ 9.34 (br s, 1H, Nb-*H*), 7.11 (s, 2H, *o*-Ar), 7.03 (s, 2H, *o*-Ar), 6.62 (s, 1H, *p*-Ar), 6.57 (s, 1H, *p*-Ar), 6.54 (s, 1H, *p*-Ar), 6.14 (s, 2H, *o*-Ar), 4.30 (s, 2H, N-CH_2), 2.70 (d, 1H, J = 13 Hz, N-CH_2), 2.62 (d, 1H, J = 13 Hz, N-CH_2), 2.33 (s, 6H, Ar-CH_3), 2.30 (s, 1H, N=C(*H*)-Ad), 2.15 (s, 6H, Ar-CH_3), 2.14 (s, 6H, Ar-CH_3), 1.90−1.66 (m, 1-Ad), 1.47−1.32 (m, 1-Ad), 1.04−0.96 (m, 1-Ad). ^{13}C{^{1}H} NMR (75.0 MHz, C_6D_6, 23 °C): δ 156.3 (aryl *ipso*), 145.5 (aryl *ipso*), 141.3 (*p*-Ar), 140.4 (*p*-Ar), 138.6 (*p*-Ar), 128.8 (aryl *ipso*), 127.4 (*m*-Ar), 125.79 (*m*-Ar), 122.8 (*m*-Ar), 117.4 (*o*-Ar), 116.8 (*o*-Ar), 115.5 (*o*-Ar), 82.7 (N=*C*(H)Ad), 68.7 (N-*C*H$_2$), 66.3 (N-*C*H$_2$), 57.8 (Ad), 44.8 (Ad), 42.3 (Ad), 41.6 (Ad), 38.3 (Ad), 38.2 (Ad), 37.6 (Ad), 37.4 (Ad), 37.3 (Ad), 36.3 (Ad), 34.7 (Ad), 30.0 (Ad), 29.4 (Ad), 29.3 (Ad), 23.1 (Ar-*C*H$_3$), 22.3 (Ar-*C*H$_3$), 22.0 (Ar-*C*H$_3$), 21.9 (Ad), 15.9 (Ad), 14.6 (Ad).

Synthesis of (O)Nb(N[CH$_2$-^{1}Ad]Ar)$_3$ ($\mathbf{1}^{CH_2Ad}$-O). To a 25 mL Teflon-stoppered Schlenk tube was added a THF solution (7 mL) of (H)Nb(η^2-^{1}Ad(H)C=NAr)(N[CH$_2$-^{1}Ad]Ar)$_2$ (125 mg, 0.14 mmol). The head space was evacuated, then backfilled with 1 atm of N_2O at 22 °C (∼1 mmol, ∼10 equiv). The solution was allowed to stir for 18 h prior to removal of all volatiles *in vacuo*. The residue was taken up in pentane/ethyl ether, and the desired product was precipitated as a white powder (that produces yellow solutions) at −35 °C in several crops. ^{1}H NMR (C_6D_6, 20 °C, 500 MHz): δ 6.56 (s, 3H, *p*-Ar), 6.49 (s, 6H, *o*-Ar), 4.33 (s, 6H, N-CH_2), 2.11 (s, 18H, Ar-CH_3), 1.95 (s, 9H, ^{1}Ad), 1.69 and 1.66 (m, 36H, ^{2}Ad) ppm. ^{13}C{^{1}H} NMR (C_6D_6, 20 °C, 125.8 MHz): δ 154.8 (*ipso*-Ar), 138.9 (*o*-Ar), 126.0 (*m*-Ar), 122.8 (*p*-Ar), 76.2 (N-*C*H$_2$), 42.1, 38.1 (NCH$_2$-*C*), 37.9, 29.6, 21.9 (Ar-*C*H$_3$) ppm.

Synthesis of the Niobaziridine Hydride Complex Nb(H)(η^2-C$_5$H$_{10}$C=NAr)(N[Cy]Ar)$_2$ ($\mathbf{2}^{Cy}$-H). Complex $\mathbf{2}^{Cy}$-H was prepared analogously to complex $\mathbf{2}^{Np}$-H employing 2.00 g (2.10 mmol) of $\mathbf{1}^{Cy}$-I$_2$ and 0.970 g (2.32 mmol, 1.10 equiv) of Mg(THF)$_3$-(anthracene). Crude $\mathbf{2}^{Cy}$-H was extracted from MgI_2 and anthracene with *n*-pentane. A filtration using thawing *n*-pentane was performed to remove residual anthracene. The product was crystallized from a mixture of Et_2O and $(Me_3Si)_2O$ over several days at −35 °C to afford $\mathbf{1}^{Cy}$-H as an orange microcrystalline solid (550 mg, 0.78 mmol, 38% yield). ^{1}H NMR (500 MHz, C_6D_6, 23 °C): δ 9.50 (br s, 1H, Nb-*H*), 7.29 (s, 2H, *p*-Ar), 6.83 (s, 4H, *o*-Ar), 6.64 (s, 2H, *o*-Ar), 6.58 (s, 1H, *p*-Ar), 3.1−3.3 (m, 4H, Cy), 2.4 (m, 2H, Cy), 2.36 (s, 6H, Ar-CH_3), 2.12 (s, 12H, Ar-CH_3), 1.8 (m, 6H, Cy), 1.4−1.6 (m, 5H, Cy), 1.15−1.4 (m, 4H, Cy), 0.85−1.2 (m, 9H, Cy), 0.65 (m, 2H, Cy) ppm.

Benzaldehyde Insertion. Synthesis of (PhCH$_2$O)Nb(η^2-C$_5$H$_{10}$C=NAr)(N[Cy]Ar)$_2$ ($\mathbf{2}^{Cy}$-OCH$_2$Ph). At 22 °C benzaldehyde (5.0 μL, 0.050 mmol, 1.05 equiv) was added to an Et_2O solution (2 mL) of orange (H)Nb(η^2-C$_6$H$_{10}$=NAr)(NCyAr)$_2$ (33 mg, 0.047 mmol). The solution immediately lightened slightly to yellow. After 30 min the solvent was removed *in vacuo* to reveal a yellow powder. ^{1}H NMR (C_6D_6, 20 °C, 500 MHz): δ 7.34 (d, J=8 Hz, 2H, *o*-Ph), 7.26 (t, J=6 Hz, 2H, *m*-Ph), 7.22 (s, 2H, *p*-Ar), 7.16 (t, 1H, *p*-Ph), 6.75 (s, 4H, *o*-Ar), 6.66 (s, 2H, *o*-Ar), 6.60 (s, 1H, *p*-Ar), 5.65 (s, 2H, Ph-CH_2), 3.85 (m, 2H, Cy), 3.15 (m, 2H, Cy), 2.36 (s, 6H, Ar-CH_3), 2.14 (s, 12H, Ar-CH_3), 1.7−2.0 (m, 11H, Cy), 1.57 (m, 4H, Cy), 1.25−1.45 (m, 5H, Cy), 1.0−1.2 (m, 6H), 0.6−0.8 (m, 2H, Cy) ppm. ^{13}C{^{1}H} NMR (C_6D_6, 20 °C, 125.8 MHz): δ 151.1, 147.1, 143.1, 139.0, 138.2, 138.0, 128.9, 127.8, 127.6, 127.5, 122.6, 117.7, 76.0 (ArN-*C*), 74.5(ArN=*C*), 64.7 (Ph*C*H$_2$O), 36.0, 35.5, 35.0, 27.8, 27.3, 26.9, 26.7, 26.1, 22.3 (Ar-*C*H$_3$), 21.8 (Ar-*C*H$_3$) ppm.

Synthesis of ONb(NCy$_2$)$_3$. Solid $LiNCy_2$ (7.0 g, 59.3 mmol, 3.04 equiv) was added to a thawing Et_2O slurry (100 mL) of $ONbCl_3(THF)_2$ (7.0 g, 19.5 mmol, 1 equiv). The color of the mixture changed from white to purple and then brown over the course of the addition and the following 2.5 h, over which time it was stirred while warming to 23 °C. After this time, the mixture was filtered through Celite and then dried *in vacuo*. The residue was extracted with a pentane/toluene mixture and filtered once more. Precipitation from 30 mL of pentane at −35 °C afforded the desired product as an off-white powder (4.95 g, 40% yield). Crystallization from toluene/Et_2O affords a bright white powder. ^{1}H NMR (C_6D_6, 20 °C, 500 MHz): δ 3.01 (m, 6H, N-C*H*), 1.89 (m, 12H, Cy), 1.79 (dd, 24H, Cy), 1.57 (d, 6H, Cy), 1.32 (q, 12H, Cy), 1.18 (t, 6H, Cy) ppm. ^{13}C NMR (C_6D_6, 20 °C, 125.8 MHz): δ 60.1 (N*C*), 37.2, 27.7, 26.4 ppm. Anal. Calcd for $C_{36}H_{66}N_3ONb$: C, 66.54; H, 10.24; N, 6.47. Found: C, 66.74; H, 10.02; N, 6.48.

Synthesis of (TfO)$_2$Nb(NCy$_2$)$_3$. To a ca. −50 °C yellow-brown solution of ONb(NCy$_2$)$_3$ (2.9 g, 4.46 mmol) in Et_2O (80 mL) was added a −35 °C solution of Tf_2O (1.25 g, 4.43 mmol, 0.98 mmol) in Et_2O (10 mL). Upon addition, the solution turned bright yellow concomitant with the formation of a yellow precipitate. After stirring for 30 min, the solids were filtered off and washed with pentane to afford the desired product (3.6 g, 3.86 mmol, 87% yield). ^{1}H NMR (C_6D_6, 20 °C, 500 MHz): δ 4.86 (m, 6H), 2.24 (m, 12H), 1.79 (m, 12H), 1.58 (m, 30H), 0.97 (m, 6H) ppm. ^{13}C NMR (C_6D_6, 20 °C, 125.8 MHz): δ 65.6 (N-*C*H), 36.2 (Cy), 27.7(Cy), 26.2 (Cy) ppm. Anal. Calcd for $C_{38}H_{66}N_3O_6F_6S_2Nb$: C, 48.97; H, 7.14; N, 4.51. Found: C, 48.66; H, 6.87; N, 4.30.

Synthesis of Nb(H)(η^2-C$_5$H$_{10}$C=NCy)(NCy$_2$)$_2$ ($\mathbf{2}^{Cy2}$-H). To a thawing THF solution of (TfO)$_2$Nb(NCy$_2$)$_3$ (250 mg, 0.27 mmol) was added magnesium anthracene tris(tetrahydrofuran) (125 mg, 0.30 mmol, 1.1 equiv) solid in small portions. After the addition, the mixture was allowed to stir for ∼45 min prior to removal of

solvent and a thawing pentane extraction of the residue with filtration through chilled Celite to remove anthracene and salts. The filtrate was dried *in vacuo* to give a nice orange powder, which could be recrystallized from Et_2O/hexamethyldisiloxane in good yield (ca. 70%). ^{1}H NMR (C_6D_6, 20 °C, 500 MHz): δ 9.0 (br s, Nb*H*, 1H), 2.88 (m, 2H), 2.69 (pseudo-t, 1H), 2.46 (m, 2H), 1.0−2.1 (m, 60H) ppm. ^{13}C NMR (C_6D_6, 20 °C, 125.8 MHz): δ 73.4 (N=*C*), 63.8 (N-*C*H), 53.7 (N-*C*H), 40.5, 38.9, 38.3, 37.3, 28.6, 27.45, 27.35, 27.3, 27.2, 26.5, 26.4 ppm.

Benzaldehyde Insertion into Nb(H)(η^2-C_5H_{10}C=NCy)(NCy_2)$_2$ (2^{Cy2}-OCH_2Ph). Synthesis of ($PhCH_2O$)Nb(η^2-C_5H_{10}C=NCy)(NCy_2)$_2$. At −35 °C, an Et_2O solution (2 mL) of benzaldehyde (22 mg, 0.21 mmol, 1.0 equiv) was added to an Et_2O solution (4 mL) of orange Nb(H)(η^2-C_5H_{10}C=NCy)(NCy_2)$_2$ (130 mg, 0.21 mmol). The solution immediately lightened slightly to yellow. After 30 min the solvent was removed *in vacuo* to reveal a yellow powder. ^{1}H NMR (C_6D_6, 20 °C, 300 MHz): δ 7.78 (d, J = 7 Hz, 2H, *o*-Ph), 7.27 (t, J = 7 Hz, 2H, *m*-Ph), 7.13 (t, 1H, *p*-Ph), 5.73 (s, 2H, Ph-CH_2), 3.71 (m, 1H), 3.2 (m, 4H), 2.69 (m, 2H), 2.45 (m, 2H), 2.15 (m, 2H), 1.0−2.0 (m, 54H) ppm.

Reduction of Nb(H)(η^2-*t*-Bu(H)C=NAr)(N[Np]Ar)$_2$. To a 3:1 Et_2O/THF (5 mL) solution of 2^{Np}-H (100 mg, 0.15 mmol) was added a slurry of KC_8 (22 mg, 0.16 mmol, 1.1 equiv) in Et_2O at −35 °C. An immediate color change to emerald green ensued. An aliquot of this reaction was analyzed by EPR spectroscopy to reveal a 10-line pattern indicative of d^1 Nb(IV). EPR (X-band, THF, 293 K): g_{iso} = 1.97, A_{iso}(^{93}Nb) = 110 G. On one occasion crystals of green [(THF)$_3$Na][Nb(H)(η^2-*t*-Bu(H)C=NAr)(N[Np]Ar)$_2$] were obtained from the reaction mixture of 1^{Np}-OTf_2 and 1% Na/Hg following removal of 2^{Np}-H by pentane extraction and crystallization of the green byproduct from Et_2O at −35 °C.

Acknowledgment. We gratefully thank the USA National Science Foundation for financial support (CHE-719157) and for a predoctoral fellowship to N.A.P.

Supporting Information Available: Full experimental and spectroscopic details for all new compounds, results of crystallographic structure determinations, computational and electrochemical studies and kinetics data (PDF and CIF). This material is available free of charge via the Internet at http://pubs.acs.org.